



1 **Simulation of Surface Fluxes in Two Distinct Environments along a Topographic**
2 **Gradient in a Central Amazonian Forest using the INtegrated LAND Surface Model**

3
4
5
6
7
8
9
10
11
12
13
14
15
16
17
18
19
20
21
22

Elisângela Broedel¹, Celso von Randow¹, Luz Adriana Cuartas², Antônio Donato Nobre⁶, Alessandro Carioca de
Araújo⁴, Bart Kruijt³, Etienne Tourigny⁵, Luiz Antônio Cândido⁶, Martin Hodnett⁷, Javier Tomasella¹

¹ *Earth System Science Center, National Institute for Space Research (INPE), São José dos Campos, Brazil.*

² *Brazilian Center for Monitoring and Warning of Natural Disasters (CEMADEN), São José dos Campos, Brazil.*

³ *Alterra Research Institute, Wageningen University, Wageningen, Netherlands.*

⁴ *Brazilian Agricultural Research Corporation (EMBRAPA), Belém, Brazil.*

⁵ *Barcelona Supercomputing Center (BSC), Barcelona, Spain.*

⁶ *Large Scale Biosphere-Atmosphere Experiment in Amazônia (LBA), National Institute for Amazonian Research (INPA),
Manaus, Amazonas, Brazil.*

⁷ *Centre for Ecology and Hydrology, Wallingford, Oxfordshire, United Kingdom.*

23

Abstract

24
25
26
27
28
29
30
31
32
33
34
35
36
37
38

The Integrated Land Surface model (INLAND) land surface model, in offline mode, was adjusted and forced with prescribed climate to represent two contrasting environments along a topographic gradient in a central Amazon *Terra Firme* forest, which is distinguished by well-drained, flat plateaus and poorly drained, broad river valleys. To correctly simulate the valley area, a lumped unconfined aquifer model was included in the INLAND model to represent the water table dynamics and results show reasonable agreement with observations. Field data from both areas are used to evaluate the model simulations of energy, water and carbon fluxes. The model is able to characterize with good accuracy the main differences that appear in the seasonal energy and carbon partitioning of plateau and valley fluxes, which are related to features of the vegetation associated with soils and topography. The simulated latent heat flux (LE) and net ecosystem exchange of carbon (NEE), for example, are higher on the plateau area while at the bottom of the valley the sensible heat flux (H) is noticeably higher than at the plateau, in agreement with observed data. Differences in simulated hydrological fluxes are also linked to the topography, showing a higher surface runoff (R) and lower evapotranspiration (ET) in the valley area. The different behavior of the fluxes on both annual



39 and diurnal time scales confirms the benefit of a tiling mechanism in the presence of large
40 contrast and the importance to incorporate subgrid-scale variability by including relief
41 attributes of topography, soil and vegetation to better representing *Terra Firme* forests in
42 land surface models.

43

44 **Key words:** Landscape heterogeneity; plateau; valley; land surface model; water balance;
45 carbon balance; central Amazon; *Terra Firme* forest soil and vegetation parameters.

46

47 1. Introduction

48 The Amazon Rainforest, which has an area of more than 6.3 million km², contains
49 approximately 50% of the world's tropical forests (Pan et al., 2011). The region is a mosaic of
50 landscapes which are traditionally divided into two major forest types: inundated (over
51 alluvial terrain) and non-inundated upland (*Terra Firme*) forests (Prance et al., 1979). *Terra*
52 *Firme* forests are found in well-drained areas with an elevation lower than 100 m; these
53 forests cover a high percentage of the Amazon. In the central region, for example, *Terra*
54 *Firme* forests represent 80% to 90% of the area (Ayres, 1995, Hess et al., 2003) or perhaps
55 more (Anderson et al., 2009). Furthermore, these forests contain approximately 74% of the
56 terrestrial biomass in the Brazilian Amazon basin (Vieira et al., 2004), including complex
57 strata of emergent trees, canopy trees, understory trees, understory shrubs, saplings, seedlings,
58 herbs and ferns. When viewed on a large scale, Amazonian *Terra Firme* forests appear to
59 form a homogeneous plain that is structurally uniform. However, when analyzed at a smaller
60 scale (spatial scales on the order of tens of meters to a few kilometers), there are diverse
61 environments that are determined by topography, soil type and soil moisture regime that are
62 often masked by dense forest cover (Nobre et al., 2011). In the central Amazon, a relatively
63 small area of *Terra Firme* forest usually comprises the topographic gradient of the plateau,
64 slope and valley environments (Chauvel et al., 1987; Araújo et al., 2010; Hodnett et al., 1997,
65 Nobre et al., 2011; Rennó et al., 2008). These environments are characterized by a high
66 variability in species composition, which is at odds with the homogeneous appearance found
67 in satellite images. The plateaus are approximately 50 to 90 m higher than the valley bottoms,
68 with moderately steep slopes between them. The valley bottom areas are swampy, with pools
69 of water and small streams which are locally known as *Igarapés* (Chauvel et al., 1987).
70 Groundwater from beneath the plateau and slopes continuously flows to the valley where it



71 maintains the water table close to the surface, even in most dry seasons (Hodnett et al., 1997).
72 Using this elevation range as a threshold, Anderson et al. (2009) found that 17% of the *Terra*
73 *Firme* forests in this landscape can be considered a valley vegetation type. According to
74 Nobre et al. (2011), in the central Amazon, which is representative of other extensive areas in
75 Amazonia, the valley forest environment covers 26.2% of the area, whereas the slope and
76 plateau forests occupy 30.7% and 43.1%, respectively. Miguez-Macho and Fan (2012) found,
77 using a numerical model, that the water table exists between the surface and a depth of 2 m
78 across 20 - 40% of the area of the Amazon throughout the year.

79
80 The local topographic heterogeneity is an important factor that governs the diversity of
81 elements comprising the landscape in *Terra Firme* forests (Lieberman et al., 1985; Takyu et
82 al., 2002). This topographic heterogeneity exerts a significant influence on soil composition
83 and the distribution of vegetation (Pelissier et al., 2001). The type of vegetation in each
84 topographic zone is associated with differences in leaf area index, which influences the
85 radiation balance and the gas and energy exchange between the plant environment and the
86 atmosphere (Araújo, 2009; Leitão 1994; Oliveira, 2010). Thus, the topographical
87 heterogeneity is also associated with carbon exchange changes between the forest and the
88 atmosphere (Araujo et al., 2008). The topography also affects the water content and the water
89 dynamics of the soil (Tomasella et al., 2008; Ferreira et al. 2002) and plays a decisive role in
90 the establishment of areas influencing water table variations (Cuartas et al., 2012; Nobre et
91 al., 2011). These factors affect the infiltration process and runoff as well as the amount of
92 water available in the soil for extraction by plant roots, which is associated with the
93 transpiration process (Tomasella et al., 2008). The topographic effects on hydrology, soils and
94 vegetation described here are certainly not due the topography *per se*, but to environmental
95 conditions defined by the topography. Although these fluxes can be quantified through land
96 surface models (LSMs) or soil-vegetation-atmosphere-transfer models (SVATs), their coarse
97 grid resolutions and simplified parameterizations of subgrid-scale heterogeneity induce errors
98 in the modeled mean fluxes due to the strong nonlinearity and fine-scale heterogeneity of land
99 surface processes. There are still no studies that explicitly incorporate subgrid-scale
100 variability by including relief attributes (topography), soil and vegetation to better represent
101 *Terra Firme* forests in these models. Developing models with this perspective will allow
102 progress in the representation of the Amazon basin at the large scale within integrated Earth
103 System models. However, to better understand its role in the global climate and how each
104 topographical type is associated with the effects of vegetation, soil and soil moisture



105 dynamics on the regional water budget, a better understanding of smaller-scale features is
106 needed. The main objective of the present work was to determine and characterize the
107 necessary components (including soil, vegetation and hydraulic) of the Integrated Land
108 Surface (INLAND) model to simulate the plateau and valley environments in a primary forest
109 in the central Amazon. To assess the quality of the model, we evaluated the surface fluxes
110 over a plateau and valley and compared them against *in situ* observations. We hypothesized
111 that the model would simulate the differences in fluxes between the plateaus and valleys
112 because the energy exchange dynamics of these ecosystems are different due to the large
113 diversity in their surface characteristics.

114

115 **2. Materials and methods**

116 *a. Study area description*

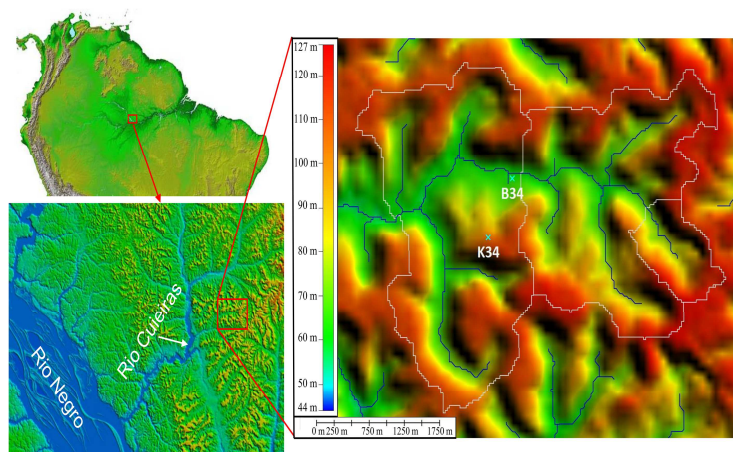
117 The study area is an instrumented hydrological catchment of 6.37 km² (54° 58'W, 2° 51'S)
118 that is located in the Cuieiras Biological Reserve, also known as ZF2, which belongs to the
119 National Institute for Amazon Research (INPA). The site is 80 km northwest of Manaus in the
120 central Brazilian Amazon rainforest (Figure 1). This site is typical of the topography of much
121 of central Amazonia and the vegetation is typical of undisturbed primary tropical forests or
122 dense *Terra Firme* forests (Ferreira et al., 2005). The climate in central Amazonia is tropical
123 rainforest climate (Af) according to the Koppen classification (Alvares et al., 2014), with
124 monthly average temperatures between 25 °C in July and 27 °C in November and an average
125 relative humidity that exceeds 80% (Leopoldo et al., 1987). The mean annual rainfall is
126 approximately 2000 mm, although it can vary from 1400 to 2800 mm. The rainy season is
127 from November to May, and a dry (or less wet) season occurs from June to October.
128 Approximately 73% of total precipitation, falls during short, heavy rainfall events (Leopoldo
129 et al., 1987).

130

131 The site area is a headwater catchment consisting of plateau areas that vary in height between
132 90 and 110 m above sea level (asl) and are strongly incised. The slopes are steep, with a
133 concave form leading to rather broad, flat valley bottoms (much narrower at the head) at 40-
134 60 m asl. Over the 6.37 km² catchment area, the valley bottoms occupy 43% of the surface,
135 and the slope and plateau areas occupy 26% and 31%, respectively (Nobre et al., 2011). The
136 vegetation cover on the plateau and slope areas is composed of tall and dense *Terra Firme*
137 (non-flooding) tropical forest, with canopy heights varying between 30 to 44 m. On the valley



138 floor, the vegetation cover is less dense, with canopy heights from 15 to 25 m (Oliveira et al.,
139 2002). The soil composition is strongly controlled by the topography and can be classified
140 into three dominant types along the topographic gradient: clayey Oxisols on the plateaus
141 (Yellow Latosols in the Brazilian system), transitioning to less clayey Ultisols on the slopes
142 (Podzol in the Brazilian system) and ending with the sandy Spodosols on the valley bottoms
143 (Chauvel et al., 1987). These soils are typically acidic and very low in nutrients such as
144 phosphorus, calcium, and potassium (Bravard and Righi, 1989). In the valley bottoms, the
145 water table remains near the surface for most of the year, often up to 100 m from the stream,
146 and these areas often contain swampy pools. A more detailed description of the site can be
147 found in Araújo et al. (2002), Waterloo et al. (2006), Cuartas et al. (2007), Luizão et al.
148 (2004) and Chambers et al. (2004).
149



150

151 **Figure 1.** Location of the study area in the Cuieiras Biological Reserve, Manaus, Amazonas, Brazil.

152

Source: Adapted from Cuartas et al. (2012)

153

154 *b. Site measurements*

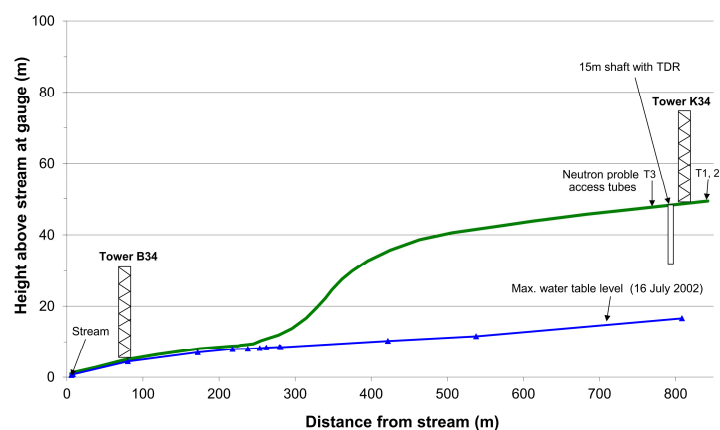
155 The datasets used in this study include meteorological and hydrological data which were
156 provided by the Large-Scale Biosphere-Atmosphere (LBA) Experiment in the Amazon
157 (Figure 2). The meteorological data were obtained from two micrometeorological eddy flux
158 towers located 600 m apart: one on the plateau and the other on the valley bottom, with an
159 elevation difference of approximately 60 m. The temporal resolution of the data used in this
160 study is 60 minutes. The plateau tower (known as K34, 2° 36'32.67"S, 60° 12'33.48"W, 54 m
161 asl) provided the data for this study from January 2000 to December 2011, including air



162 temperature ($^{\circ}\text{C}$), precipitation (mm), downward shortwave and longwave radiation (W m^{-2}),
163 wind speed (m s^{-1}), relative humidity, carbon dioxide (CO_2 , $\mu\text{ mol m}^{-2} \text{ s}^{-1}$), and latent (LE, W
164 m^{-2}) and sensible (H, W m^{-2}) heat fluxes. The valley bottom tower (known as B34, 2°
165 $36'09.8''\text{S}$, $60^{\circ} 12'44.5''\text{W}$, 42 m asl) provided data from January 2006 to December 2006,
166 including CO_2 and LE and H fluxes. All measurements were made from the top of the towers.
167 More details about the K34 and B34 tower instrumentation and the measured variables can be
168 found in Araújo et al. (2002) and Araújo (2009).

169

170 The hydrological data obtained was the soil water content in the plateau and stream discharge
171 and water table level in the valley. The soil water content ($\text{m}^3 \text{ m}^{-3}$) was obtained using two
172 instruments: neutron probe (Didcot Instrument Co., Burwell, Cambridge, UK) and time
173 domain reflectometry - TDR (Campbell Scientific Inc. CS615, Logan, Utah, USA), which are
174 both located on the plateau, approximately 30 m from the K34 meteorological tower (Figure
175 2). Neutron probe measurements were obtained from 3 access tubes (T1, T2 and T3) installed
176 from the surface to a depth of 4.8 m, with weekly or biweekly measurements from December
177 2001 to December 2006 (Cuartas et al., 2012). The soil water content was also obtained from
178 TDR sensors between depths of 0.8 to 8.0 m, which were installed along the walls of a lined
179 15 m shaft, with continuous data recording at hourly intervals between January 2003 and
180 February 2006 (Broedel et al., 2017). Furthermore, water table depth (m) and stream
181 discharge ($\text{m}^3 \text{ s}^{-1}$) data were used for the study area during the period from July 2002 to
182 October 2006. The stream discharge ($\text{m}^3 \text{ s}^{-1}$) was measured using the ultrasonic Doppler
183 technique (Starflow model 6526, UNIDATA, O'connor, Fremantle, Australia) in the valley
184 area. The water level and average and maximum discharge velocity data necessary to obtain
185 the stream discharge were logged every 30 minutes and downloaded from a data logger on a
186 weekly basis. Details on the derivation of the stream discharge data can be found in Waterloo
187 et al., (2006). The water table depth was measured weekly with 7 piezometers spread over the
188 valley area, consisting of perforated Polyvinyl Chloride (PVC) tubes with a diameter of 5 cm
189 and filters (Eijkelkamp Agrisearch Equipment, Nijverheidsstraat, Giesbeek, The Netherlands)
190 (Tomasella et al., 2008).



191

192 **Figure 2.** Topographical gradient in a tropical rain forest in the central Amazon and instrumental data. Blue
193 triangle symbols show the height of the water table at the positions of boreholes for monitoring the water table.

194

195 d. *The INLAND model*

196 Version 1.0 of the INtegrated LAND surface model (INLAND) was used in this study
197 (Tourigny, 2014). The INLAND model is a Brazilian development based on the Integrated
198 Biosphere Simulator (IBIS) model (Foley et al., 1996; Kucharik et al., 2000), including all of
199 its main features, using a modular, physically consistent framework to perform integrated
200 simulations of water, energy, and carbon fluxes, but with improvements to simulate particular
201 tropical processes. Here we discuss the components of INLAND that are most relevant to the
202 focus of this paper. The model consists of four component modules organized with respect to
203 their characteristic temporal scales: a land surface module (minutes to hours), a vegetation
204 phenology module (days to weeks), and carbon balance and vegetation dynamics modules,
205 which both have a temporal scale of years. The land surface module of INLAND is taken
206 from the second-generation LSX model (Pollard and Thompson, 1995) and includes 6 soil
207 layers (with varying thicknesses) and an upper (trees) and lower (shrubs and grasses) canopy.
208 Plants are represented by 12 plant functional types (PFTs), each with distinct carbon pools for
209 leaves, stems and roots. The Amazon basin in INLAND model is predominantly represented
210 by the *tropical broadleaf evergreen* tree PFT. The soil module in INLAND simulates soil
211 temperature, water content, and ice content (when required) in each of the 6 soil layers and
212 solves the θ -based form of the Richards equation, where the soil moisture change in time and
213 space is a function of soil water retention curve, soil hydraulic conductivity, upper and lower
214 boundary conditions and plant water uptake. The plant root-water uptake (represented by a
215 sink term in the macroscopic Richard's equation) is a function of atmospheric demand, soil



216 physical properties, root distribution, and soil moisture profile (Kucharik et al., 2000). The
217 drainage from the bottom soil layer is modeled assuming gravity drainage and neglects
218 interactions with groundwater aquifers.

219

220 Energy balance in the INLAND model is separately calculated for each surface type. Under
221 steady-state conditions, the balance between incoming and outgoing radiation or net radiation
222 at the surface (R_n) must equal the sum of sensible (H), latent (LE) and ground (G) heat fluxes,
223 heat storage within the vegetation canopy (S) and the sum of additional energy sources and
224 sinks (Q). Both S and Q are frequently neglected because of their small magnitudes. Net
225 radiant energy is partitioned between latent, sensible and ground heat fluxes following a
226 Penman-Monteith approach (for details see Monteith, 1965). The model calculates the
227 canopy-level surface carbon balance through the flow of carbon between the atmosphere and
228 plants, which is also known as the net ecosystem exchange (NEE). Negative NEE values
229 correspond to the net carbon uptake by the land surface. The NEE is computed as the
230 difference between heterotrophic respiration (R_h) and net primary productivity (NPP). NPP
231 refers to the carbon that remains stored in plants after taking up CO_2 from the atmosphere
232 during gross primary productivity (GPP) and that has partially respired back through
233 autotrophic respiration (R_a). Leaf-level photosynthesis in the model is determined by the
234 formulations of Farquhar (Farquhar et al., 1980). In these formulations, the photosynthesis
235 rates are a function of absorbed light, leaf temperature, CO_2 concentration within the leaf, and
236 the Rubisco enzyme capacity of photosynthesis. The stomatal conductance is dependent on
237 the photosynthetic rate, CO_2 concentration, and water vapor concentration (Foley et al. 1996).
238 The current version of the model uses a single-leaf photosynthesis approach, and the coupling
239 between photosynthesis and canopy conductance is based on vapor pressure deficit (Leuning,
240 1995).

241

242 *e. Development of an unconfined aquifer model*

243 The INLAND model does not explicitly represent water table dynamics. Instead, the lower
244 boundary condition is allowed to vary from 100% free drainage to zero flux (based on an
245 empirical coefficient ranging from 0 to 1). This means that the model can be applied to a
246 plateau environment, although it cannot correctly simulate a valley environment where the
247 water table remains at or very close to the soil surface for much of the year. Consequently, we
248 incorporated into the INLAND model a lumped unconfined aquifer model developed by Yeh



249 and Eltahir (2005 a, b), in which the water table is interactively coupled to the soil column
250 through the soil drainage (groundwater recharge) fluxes. All processes within INLAND,
251 except for those computing the soil moisture, were preserved with the original IBIS equations.
252 The lumped water balance equation for an unconfined groundwater aquifer can be written as
253 follows, according to Yeh and Eltahir (2005 a):

254

$$S_y \frac{dH}{dt} = I_{gw} - Q_{gw} \quad (1)$$

255

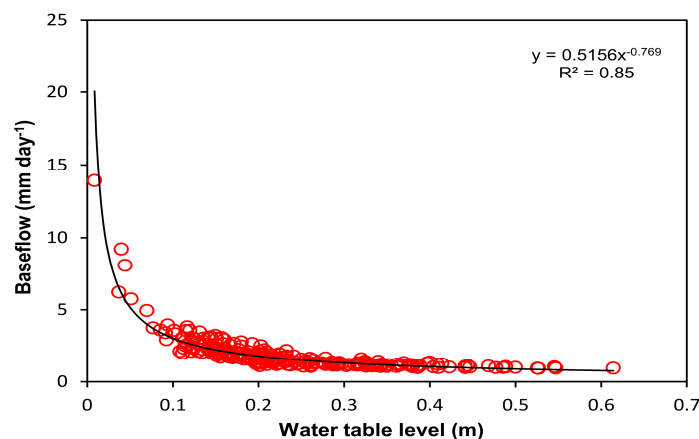
256 where S_y (dimensionless) is the specific yield of the unconfined aquifer, H (m) is the water
257 table level above the datum, I_{gw} (mm day^{-1}) is the groundwater recharge flux, which is the
258 flux at the interface between the unsaturated and saturated zone, i.e., the water table, and Q_{gw}
259 (mm day^{-1}) is the groundwater discharge to streams (i.e., groundwater runoff). For the sandy
260 soils typical of the valleys in the central Amazon rainforests, the value of S_y was specified as
261 0.265, which is based on specific yield data compiled by Johnson (1967). Yeh and Eltahir
262 (2005a) identified a strong nonlinear relationship between the baseflow discharge and water
263 table depth. A regression analysis was performed on 5 years of baseflow discharge and water
264 level data from our study site; this analysis indicated a similarly strong relationship (Eq. 4),
265 with a correlation coefficient of 0.85 (Figure 3). The baseflow was separated from the daily
266 discharge using a digital recursive filter technique (Lyne and Hollick, 1979). This method has
267 been widely used for the continuous partitioning of streamflow discharge between surface
268 runoff and baseflow because it is fast, efficient, reproducible and objective (e.g., Furey and
269 Gupta, 2001; Nathan and McMahon, 1990 and Lo et al., 2008). Yeh and Eltahir (2005 a)
270 showed that a digital recursive filter can have a high coefficient of determination (i.e., R^2) of
271 0.84, while Arnold and Allen (1999) found a coefficient of determination of 0.86.

272

$$Q_{gw} = \frac{0.5156}{(D_{gw})^{0.796}} - 1.4 \quad (2)$$

273

274 The groundwater model represented by Eq. (3) and Eq. (4) was interactively coupled with the
275 soil model in INLAND such that the total length of the active unsaturated soil column varied
276 in response to the water table depth fluctuations by keeping the number of unsaturated layers
277 variable.



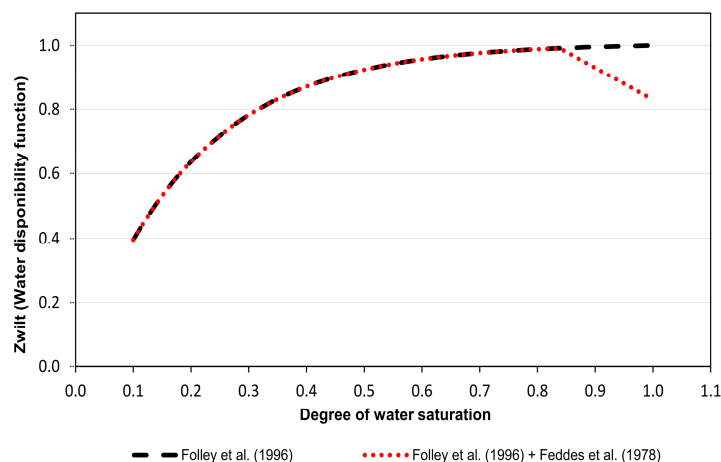
278

279 **Figure 3.** Regression analysis, including water table depth versus monthly baseflow, from July 2002 to October
280 2006 in the valley study area.

281

282 The INLAND model includes a non-linear root water extraction scheme to describe the
283 impact of soil water stress (Folley et al., 1996), in which potential transpiration is first
284 distributed over the rooted zone and then reduced to actual root-water-uptake by a soil water
285 stress reduction function. However, after incorporating the unconfined aquifer model into
286 INLAND to represent the water table dynamics of the valley site, it was also important to
287 represent the stress due to saturated (or waterlogged) conditions, which lead to oxygen
288 deficiency (hypoxia) in the soil. These conditions cannot be ignored because they influence
289 plant survival, growth and functioning at the valley sites (Pezeshki and DeLaune, 2012). We
290 used the linear function presented by Feddes et al. (1978) to describe the soil water uptake
291 reduction caused by root oxygen deficiency, which is added to Folley function (Figure 4).
292 Under optimal moisture conditions, the maximum possible root water extraction rate
293 integrated over the rooting depth is equal to the potential transpiration rate, whereas, under
294 non-optimal conditions (i.e. when the soil is either too dry or too wet) the root water
295 extraction rate may be reduced, causing a reduction in transpiration (Figure 4). For saturated
296 conditions, the reduction of root water uptake occurs between 0.83 – 1.0 degree of soil
297 saturation, which leads to a reduction of 0-17% in the plant transpiration.

298



299

300

Figure 4. The general shape of root water extraction from Folley et al. (1996) and Feddes et al. (1978) for dry and wet conditions, respectively.

301

302

303 *f. Experimental design*

304

All of the simulations reported here in were run with the single-point off-line version of the model (0D, uncoupled from a Global Circulation Model or GCM) with the CO₂ concentration set to a constant value of 400 parts per million (ppm). INLAND was forced using the observed hourly meteorological data collected at the K34 tower for 12 full years, from January 1, 2000, to December 31, 2011. For the plateau simulations, the top-to-bottom thicknesses of the 6 soil layers in INLAND were set to 0.20, 0.30, 0.50, 1.0, 2.0 and 4.0 m, resulting in a total depth of 8 m. For the valley, the total profile depth was set to 4 m, with layer thicknesses of 0.10, 0.20, 0.30, 0.40, 1.0 and 2.0 m from the top to the bottom. We conducted two sets of simulations, with a time step of 60 minutes, for each location (plateau and valley); in the first set of experiments, to avoid additional complexity, the vegetation was set to fixed, or "static", in the INLAND vegetation dynamics module. Thus, no change in the stand structure was assumed to occur during the simulation period. For simplicity, we used the same forcing data for the spin-up period, which is a preliminary simulation to equilibrate the model parameters, such as soil temperature and soil moisture. The spin-up in our simulations was done for duration of 60 years, initialized on January 1, 1940 and was discarded in the analysis. In the second set of experiments, the dynamic vegetation routine was employed in order to evaluate changes in vegetation cover (biomass stocks) and carbon fluxes (productivity) between the plateau and valley after 100 years of integration (from

321



322 January 1, 1900 to December 31, 1999). This approach consists of two different sets of
323 simulations for both the plateau and valley environments: a dynamic vegetation run, which
324 starts from initial vegetation similar to the current tropical forest biome or *dynamic vegetation*
325 *1 (DVI)*, and a “cold start” run that starts from bare soil and lets the model build the
326 vegetation cover according to climate conditions or *dynamic vegetation 2 (DV2)*. Plant
327 growth, which results from the assimilation of C through photosynthesis, contributes to the
328 formation of a canopy and is moderated by competition-related mortality. Carbon pools in
329 live and dead biomass and in the soil are continuously updated and provide a “memory” of the
330 state of the system over a series of years to decades (Folley et al. 2000).

331

332 In the original 0D version of INLAND, the values for the soil hydraulic parameters are
333 obtained from soil texture-based look-up tables commonly used in LSMs, based on pedo-
334 transfer functions (PTFs), such as those of Clapp and Hornberger (1978) and Rawls et al.
335 (1982). However, Hodnett and Tomasella (2002) showed that these PTFs, which were
336 originally derived using data from temperate region soils, do not accurately predict the
337 properties of tropical soils, particularly Oxisols. Although Oxisols have a high clay content,
338 they have low water availability and highly saturated conductivity; these characteristics differ
339 from temperate clay soils. Therefore, these look-up tables were replaced with hydraulic
340 properties for Oxisols taken from Tomasella and Hodnett (1996), Ferreira et al. (2002) and
341 Marques (2009). On the other hand, hydraulic properties for sandy soils located in valley area
342 was taken from Campbell and Norman (1998) and Verhoef and Egea (2014). Furthermore,
343 different soil hydraulic parameters were used for each layer of the soil profile. The
344 performance of the INLAND model was evaluated by comparing the simulations against the
345 observational data from both the plateau and valley areas, including LE, H, Rn, NEE, soil
346 moisture and water table level; three indices of error statistics were used (Ambrose and
347 Roesch, 1982): bias, coefficient of determination (R^2), and the Root Mean Square Error
348 (RMSE).

349

350 **3. Results and discussion**

351 *a. Representation of water table dynamics in the valley*

352

353 After identifying the optimal vegetation and soil parameters set of plateau and valley forest
354 (Table 1), and incorporating the unconfined aquifer model into INLAND to correct represent

355 the valley area, we compared the water table depth (WTD) simulated by model with
 356 observations, from 2002 to 2006.

357

358 **Table 1.** Vegetation and soil parameters used in the INLAND simulations for the Plateau and Valley. The initial
 359 values refer to the parameters used by Imbuzeiro (2005).

Parameter	Description	Unit	Initial	Plateau	Valley
Vegetation					
fl	Fraction of overall area covered - lower canopy	-	1.00	1.00	0.90
fu	Fraction of overall area covered - upper canopy	-	0.50	0.50	0.60
dispuhf	Zero-plane displacement height - upper canopy	m	0.70	0.70	0.60
rhoevveg_NIR	Reflectance of an avg leaf/stem near infrared - upper canopy	-	0.400	0.310	0.260
plaeivgr	Initial total LAI - upper canopy	m ² m ⁻²	5.00	4.60	4.30
ztop	Canopy height	m	30	35	18
beta1	Parameter for Jackson rooting profile - lower canopy	-	0.950	0.950	0.940
beta2	Parameter for Jackson rooting profile - upper canopy	-	0.975	0.970	0.965
V _{max}	Maximum Rubisco capacity of the top canopy at 15°C	mol CO ₂ m ⁻² s ⁻¹	80x10 ⁶	80x10 ⁶	70x10 ⁶
coefm	m coefficient for stomatal conductance relationship	-	8.0	9.0	7.5
tauleaf	Foliar biomass turnover time constant	years	1.01	1.02	1.01
tauwood0	Wood biomass turnover time constant	years	25.0	45.0	35.0
tempvm	Stress maximum coefficient of V _{max}	-	3500	6000	4500
tdripu	Decay time of liquid intercepted by leaves - upper canopy	s	7200	16200	10800
tdrips	Decay time of liquid intercepted by stems - upper canopy	s	7200	16200	10800
tdripl	Decay time of liquid intercepted by leaves and stem - lower canopy	s	7200	16200	10800
Soil					
swilt	Wilting point	m ³ m ⁻³	0.272	0.370	0.030
suction	Air entry potential	m _{H₂O}	0.370	0.100	0.050
sfield	Field capacity	m ³ m ⁻³	0.369	0.430	0.090
poros	Porosity	m ³ m ⁻³	0.475	0.48; 0.52; 0.52; 0.575; 0.59; 0.595	0.40; 0.41; 0.42; 0.43; 0.44; 0.45
bex	Campbell 'b' exponent	-	7.60	7.6 8.0; 10.0; 11.3; 13.1; 16.5	10.0
hydraul	Saturated hydraulic conductivity	m s ⁻¹	1.66x10 ⁻⁷	9.99x10 ⁻⁶	9.99x10 ⁻⁸ ; 9.99x10 ⁻⁷ ; 9.99x10 ⁻⁶ ; 9.99x10 ⁻⁵

360

361

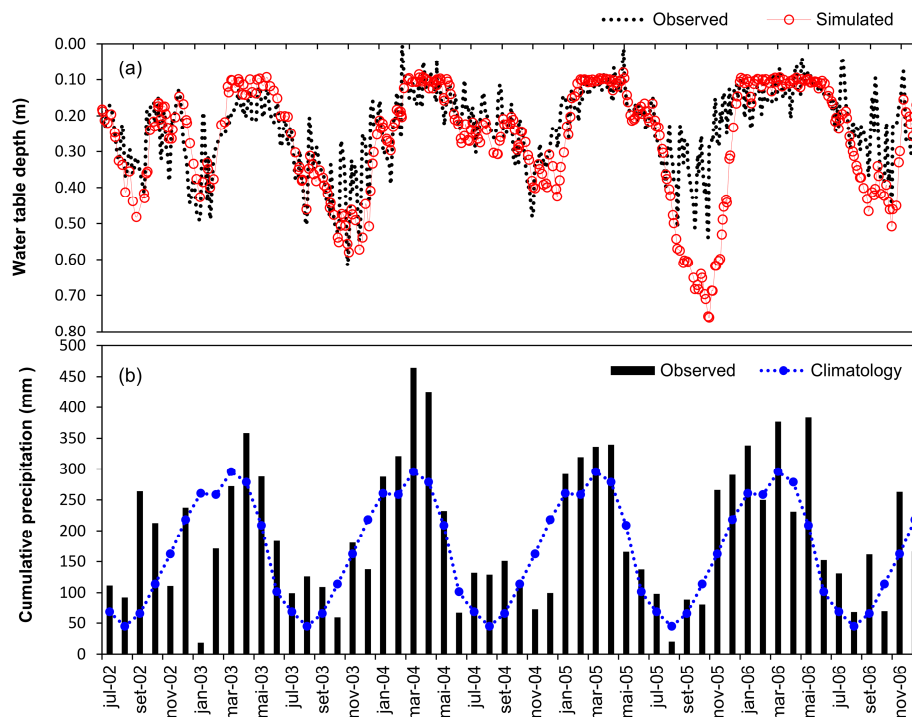
362 In general, the simulations reproduced the observed weekly or biweekly variability in the
 363 WTD reasonably well, indicating distinct seasonality and interannual variations over the
 364 studied years, with primarily very shallow WTDs in the valley environment (Figure 5a).
 365 Seasonal and interannual variability are a response to the seasonality of precipitation at the
 366 study site (Figure 5b). As soon as the rainy season begins in November, the simulated WTD
 367 decreases, with minimum values generally recorded in May, according to observed data. On
 368 the other hand, the maximum simulated WTD were recorded at the end of the dry season
 369 (September-October) or in the early wet season of next year (November), consistent as
 370 observed data. The observed data showed two strong drought events with maximum reduction
 371 of the depth of the water table, during the period analyzed. In the early wet season of 2003,
 372 the water table fell below 0.61 m from the surface (Table 2). This decrease was due to the
 373 lower annual precipitation (33% less than 2002), which was associated with the occurrence of
 374 a moderate El Niño event that influenced the Amazonian region between the end of 2002 and



375 2003 (Climanálise, 2003). Previous studies have documented the association between El Niño
376 events and precipitation reduction in Amazonia (Marengo, 2004). In the dry season of 2003,
377 the mean observed values were underestimated by the model by less than 9%. Another
378 drought event occurred two years later, when a significant rainfall deficit resulted in an
379 exceptional drought during the dry season of 2005 (Marengo *et al.*, 2008; Tomasella *et al.*,
380 2010), with values up to 50% below the climatological mean in August (Figure 5b).

381

382 During this period, the WTD observed fell below 0.54 m from the surface and the model
383 overestimated the observed WTD by approximately 40%. Although WTD showed a larger
384 decrease during the dry season of 2003, the data indicate a higher rainfall deficit in 2005
385 when the total accumulated was only 393.6 mm, about 32% lower than the presented value
386 during the same period in 2003. This result suggest for this year the INLAND model “dried
387 out” more rapidly than indicated by the observations, highlighting the limited capacity of
388 INLAND to reproduce the abrupt change from wet to dry conditions for the studied area. On
389 the other hand, in the normal years the INLAND simulated very well the transition between
390 wet to dry conditions, indicating a good agreement with observation data. The minimum
391 WTD simulated was found during the wet season of 2004/2005, about 0.08m, while in the
392 same period the observed data indicated the water table closer the surface at 0.01m. The
393 observed and simulated mean WTD in all periods were 0.21 and 0.22 m, respectively, below
394 the surface during the rainy season (November-May), increasing to 0.26 and 0.31 m below the
395 surface at the onset of the dry season (June-October) (Table 2). In general, the observed
396 values were slightly overestimated by the model (Table 3), except in the wet season of
397 2002/2003 (RMSE = 0.08 m; $R^2 = 0.65$) and dry season of 2003 (RMSE = 0.06 m; $R^2 = 0.79$).
398 The overestimation was higher in the dry season of 2005 (0.11 m) with higher RMSE (0.18m)
399 and lower R^2 (0.52). On the other hand, a better agreement was found during the wet season
400 of 2004/2005 with biases of 0.01 m, RMSE of 0.07 m and R^2 of 0.76. The overestimation of
401 the INLAND simulations during 2002-2006 was less compared to that of the Community
402 Land Model (CLM) presented in Fan and Miguez-Macho (2010) at the same study site.
403 According to the authors, the CLM model produced a water table that was 2 m too low
404 compared to the observations. Cuartas *et al.* (2012) also verified an overestimation of the
405 WTDs simulated using the Distributed Hydrology Soil Vegetation Model (DHSVM) at the
406 same study site, with an RMSE of 0.25 m during both the wet and dry seasons (2002-2006)
407 and an R^2 of 0.60 and 0.72 in the wet and dry seasons, respectively.



408

409

410

411

412

413

414

415

Figure 5. (a) Observed and simulated water table depth fluctuations in the valley area from July 2002 to December 2006; (b) Observed precipitation during the same period (vertical bars) and climatological mean precipitation between 1901-1999 in the city of Manaus (dashed line and blue dots).

Table 2. Mean, maximum and minimum water table depth from 2002 to 2006, in the valley area.

	Water table depth (m)					
	Observed			Simulated		
	Mean	Maximum	Minimum	Mean	Maximum	Minimum
Wet season 2002-2003	0.25	0.49	0.12	0.20	0.43	0.10
Wet season 2003-2004	0.22	0.61	0.01	0.25	0.58	0.09
Wet season 2004-2005	0.20	0.48	0.01	0.21	0.43	0.08
Wet season 2005-2006	0.16	0.54	0.04	0.23	0.76	0.09
Total	0.21	0.61	0.01	0.22	0.76	0.08
Dry season 2002	0.26	0.41	0.16	0.31	0.48	0.18
Dry season 2003	0.33	0.53	0.12	0.33	0.55	0.09
Dry season 2004	0.22	0.34	0.12	0.23	0.30	0.10
Dry season 2005	0.29	0.51	0.14	0.40	0.71	0.10
Dry season 2006	0.22	0.45	0.04	0.29	0.51	0.10
Total	0.26	0.53	0.04	0.31	0.71	0.09

416



417

418

Table 3. Performance of the INLAND model in representing the depth of the water table in lowland forest,
located in the study area, during the period from 2002 to 2006.

419

	Water table depth (m)		
	Bias	RMSE	R ²
Wet season 2002-2003	-0.05	0.08	0.65
Wet season 2003-2004	0.03	0.09	0.68
Wet season 2004-2005	0.01	0.07	0.71
Wet season 2005-2006	0.07	0.18	0.52
Total	0.02	0.11	0.46
Dry season 2002	0.04	0.07	0.66
Dry season 2003	-0.003	0.06	0.79
Dry season 2004	0.01	0.04	0.57
Dry season 2005	0.11	0.18	0.52
Dry season 2006	0.07	0.10	0.58
Total	0.05	0.11	0.54

420

421

422 *b. Soil moisture characteristic curves on the plateau*

423

424 Both the magnitude and seasonal amplitude variations are apparent in the model simulations
425 and observations throughout the monitored soil profile from December 2001 to December
426 2006 (Figure 6). The observational data for the deepest layer (obtained by TDR), which was
427 obtained at an hourly temporal frequency, is represented here using weekly or biweekly
428 temporal frequencies to match the observational data from the first 5 layers (neutron probe)
429 from January 2003 to February 2006. Six soil parameters (Table 1) or the model were
430 modified according to available literature in the study region (Tomasella and Hodnett, 1996;
431 Ferreira et al., 2002; Marques, 2009). The sensitivity of the model to these soil parameters
432 was examined through several simulations using different soil parameter values. Based on our
433 simulations, the three most significant parameters were porosity (*poros*), Campbell's
434 parameter (*bex*) and hydraulic conductivity (*hydraul*). For the baseline simulations, the *poros*
435 and *bex* values were allowed to vary with depth according to measurements reported in Table
436 1. The corresponding statistical performances indices are included in Table 4. The simulated
437 soil moisture content followed an annual cycle, with decreasing amplitude in the deep layers.
438 In the first 4 soil layers, the variability in the soil moisture between the dry and wet season
439 was more pronounced, compared to the other layers. This behavior was related to a rapid



440 response to precipitation in the top soil layers and to high macroporosity. At greater depths,
441 the response to rain events was damped, particularly in the last 2 layers, which responded
442 only to the seasonal variability in precipitation.

443

444 In general, the model underestimated the soil moisture content with an RMSE of $0.017 \text{ m}^3 \text{ m}^{-3}$
445 and R^2 of 0.54 for the first layer and RMSE of $0.006 \text{ m}^3 \text{ m}^{-3}$ and R^2 of 0.71 for the sixth layer.
446 The RMSE decreased and R^2 increased with depth to the sixth layer, suggesting that minor
447 errors occurred between the fifth and sixth soil layers, where the smallest soil moisture
448 variation was observed. This behavior can be explained by the high microporosity and low
449 permeability of the deep soil layers, which are responsible for slow percolation at deeper
450 depths (Nortcliff and Thornes, 1981). The lower variation in soil moisture on a seasonal scale
451 in the last 2 layers may reflect a minor presence of roots at this depth and less water. This
452 finding indicates that there was no significant extraction of water from the roots at these
453 depths because there was sufficient water in the layers above 400 cm during most years
454 (Broedel et al., 2017). The sixth layer, for example (depth of 4.00-8.00 m), had a nearly
455 constant water content of $0.57 \text{ m}^3 \text{ m}^{-3}$. An interesting behavior that was noticed in our
456 simulations was the underestimation of soil moisture in the dry season of 2005 in all of the
457 layers of the profile, suggesting that the model had difficulty simulating the extremely dry
458 conditions of the study area during this period. The observational data also indicated that the
459 depletion of soil moisture was more pronounced and lasted longer during the 2005 dry season
460 over the entire soil profile because root uptake during that period was more intense than in
461 normal years. Discrepancies in the water content at the end of the dry season of 2005 between
462 the observational and simulated results could be due to differences in the actual versus
463 assumed root distributions.

464

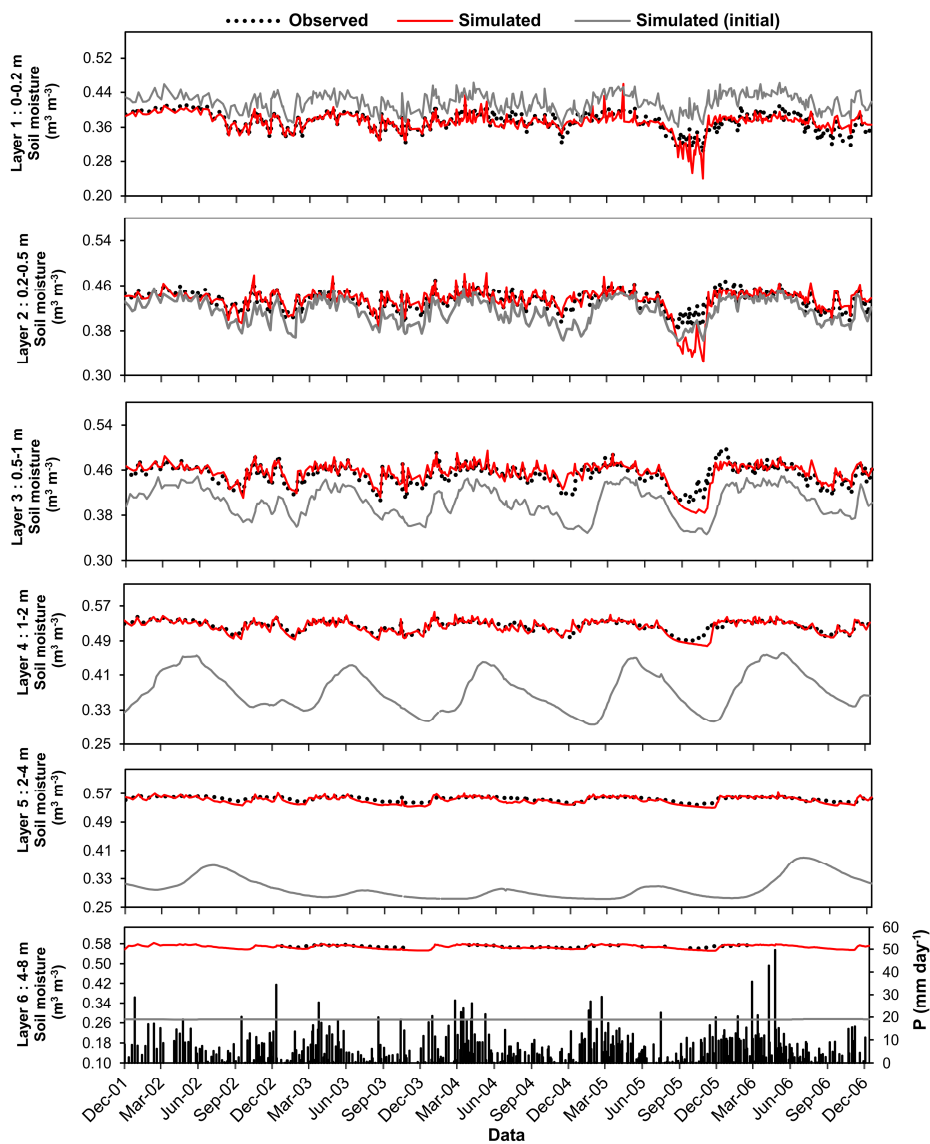
465 **Table 4.** The RMSE, bias and R^2 calculated from weekly or biweekly soil moisture data.

Layer (m)	N°	RMSE (m^3m^{-3})	Bias (m^3m^{-3})	R^2 -
0.0-0.2	1	0.017	-0.004	0.54
0.2-0.5	2	0.014	-0.001	0.65
0.5-1.0	3	0.012	0.003	0.70
1.0-2.0	4	0.008	-0.002	0.79
2.0-4.0	5	0.007	-0.004	0.72
4.0-8.0	6	0.006	-0.003	0.71

466

467

468



469

470 **Figure 6.** Observed and simulated soil moisture results for the full profile on the plateau. The observational data
 471 have a weekly or biweekly temporal frequency. Layers 1- 5: from December 2001 to December 2006, obtained
 472 from neutron sonde; Layer 6: from January 2003 to February 2006, obtained from TDR.

473

474 *c. Water balance on the plateau and in the valley*

475



476 The INLAND model simulated very well the difference of ET fluxes between plateau and
477 valley, showing larger values on the plateau than that in the valley, in accordance with the
478 observed data in 2006 (Figure 7a). The simulated annual mean ET was 3.7 mm day^{-1} and 3.2
479 mm day^{-1} for the plateau and the valley, respectively, values close to the observed data, from
480 3.0 mm day^{-1} in the plateau and 2.9 mm day^{-1} in the valley. Similar results for the plateau area
481 in the same region of study during 2000-2008 were found by Broedel (2012) - 3.6 mm day^{-1}
482 in the calibration of the CLM model - and by Assunção (2011) - 3.5 mm day^{-1} . In addition,
483 the mean ET found in this study for the plateau area also corroborates both the ET value of
484 $3.8 \text{ mm mm day}^{-1}$ estimated by Tomasella et al. (2008), for a four years subset of the data
485 series observed, using the Penman-Monteith method, and a value of 3.7 mm day^{-1} , reported by
486 Shuttleworth (1988). The difference in the ET along a topographic profile was also verified
487 by Hodnett et al. (1997a), who estimated ET in two different locations in a forest in the
488 central Amazon, i.e., on a plateau and slope (between a plateau and valley) using the water
489 balance method and found values of 3.8 mm day^{-1} and 3.6 mm day^{-1} , respectively. According
490 to Zanchi (2013), the water extraction in poorly drained valleys occurs at a shallower depth
491 and can be reduced compared with that on plateaus. Hodnett et al. (1997a) determined that the
492 extraction of water from the soil when the water table is near the surface is small (0.5 to 1 mm
493 day^{-1}) compared with the value obtained when the water table is below 1 m depth (3 mm day^{-1}).
494 1 .

495

496 The model was also able to simulate the seasonal patterns of the water balance components
497 between the plateau and valley with good accuracy. In both areas, there was a minimum in the
498 simulated ET during the wet season (plateau: 3.3 mm day^{-1} ; valley: 3.0 mm day^{-1}) that rose in
499 the dry season (plateau: 4.3 mm day^{-1} ; valley: 3.6 mm day^{-1}), compared to observed data in
500 wet (plateau: 2.5 mm day^{-1} ; valley: 2.4 mm day^{-1}) and dry (plateau: 3.6 mm day^{-1} ; valley: 3.2
501 mm day^{-1}) season. Da Rocha et al. (2009), in central Amazonia, also described a progressive
502 increase (by 10%) in ET during the dry season when compared to the wet season (2.8 mm day^{-1}),
503 and was dominated by a net radiation and vapor density deficit in a plateau area. All the
504 observed ET values were overestimated by INLAND during the entire simulated period, in
505 both areas. However, these estimations are probably lower than the real ET levels because of
506 the problem of the energy balance closure of the eddy covariance systems in tropical forests
507 (Twine et al. 2000; Wilson et al. 2002; Von Randow et al. 2004), mainly in the valley area
508 during the wet season. The bias values indicate a better agreement between simulated and
509 observed curves in the valley area (dry season = 0.4 mm day^{-1} , wet season = 0.2 mm day^{-1})



510 when compared to the plateau (dry season = 0.7 mm day⁻¹; wet season = 0.9 mm day⁻¹) (Table
511 5). In the plateau area, the highest R² values were found both in the wet season (0.71) and in
512 the dry season (0.64), indicating a better correspondence between observed and simulated
513 data when compared to valley (wet season = 0.63; dry season = 0.56). In addition, RMSE
514 values for the plateau during the dry and wet season were 1.1 mm day⁻¹ and 1.0 mm day⁻¹,
515 respectively, values similar to those found in the valley during the dry (0, 8 mm dia-1) and
516 wet (1.1 mm day⁻¹) season.

517

518 Mean ET over 2006 corresponded to 55.7% and 45.4% of precipitation in the plateau and
519 shallow areas, respectively. These values are close to those found by Tomasella et al (2008) in
520 the study area of 53%, during the period from 2001 to 2004. In addition, they are also similar
521 to the values of 50% found by Assunção (2011) in the calibration of the IBIS model and
522 56.9% obtained by Cuartas et al. (2012) using the hydrological model DHSVM, both in the
523 same study area. Of the total loss by ET, 76% were due to transpiration in both forest areas.
524 On the other hand, the evaporation of the intercepted water (interception loss) represented
525 21.2% and 19.2% in the plateau and valley, respectively, while 2.5% and 3.8% were
526 associated with direct evaporation of the soil, respectively, in the plateau and valley. These
527 results show that in the valley area, water interception by the canopy was slightly lower than
528 in the plateau (10.4%), while soil evaporation was about 52% higher than the plateau.
529 Together these results reflect the structural attributes of the vegetation in this area,
530 characterized by a greater spacing between plants, which shows a more open canopy when
531 compared to the plateau (Nobre et al, 1989), lower trees (Ranzani, 1980; Pinheiro, 2007), a
532 smaller LAI (Cuartas et al., 2012) and different tree composition with less species (Ribeiro et
533 al., 1999; Oliveira and Amaral, 2004). The INLAND model was able to simulate very well
534 the differences between the vegetation in both the areas, including a LAI of 6.1 m² m⁻² in the
535 plateau area and 5.8 m² m⁻² in the basin, in agreement with available literature (Cuartas et al.,
536 2012; Marques-Filho et al., 2005). The evaporation of intercepted water corresponded to
537 11.2% and 9.0% of precipitation, in the plateau and valley area, respectively. These values are
538 comparable to the 11% estimate obtained by Tomasella et al. (2008) for the period 2001-
539 2004, in the same experimental area. The same behavior was also observed in the estimate by
540 Shuttleworth (1988) of 12.4%, carried out in the forest of the Ducke Reserve, in Manaus, near
541 the study area. However, it is higher than the value reported by Lloyd et al. (1988) of 8.9%, in
542 the field experiment also in the Ducke Reserve and the value of 8.2% found by Assunção
543 (2011) in the study area used in the present study. In addition, the values simulated by



544 INLAND for plateau and valley are much lower when compared to 16.5% found by Cuartas
545 et al (2007), in the same study area. On the other hand, soil evaporation represented a small
546 part of the total precipitation, only about 1.3% (plateau) and 1.7% (valley), lower than that
547 found by Drucker (2001) of 2.2%, in a hydrological modeling study in the central region of
548 the Amazon, near the experimental site. According to Luizão (1989), there is almost no
549 evaporation of the soil under *terra firme* forest, which explains its lack of consideration in
550 many studies on hydrological modeling in the Amazon, such as that of Tomasella et al.
551 (2008).

552

553 The surface runoff (R) simulated by INLAND on both areas was reproduced relatively well
554 by INLAND during the period from 2002 to 2006. Simulated R in the valley was larger over
555 the entire simulation compared with the plateau (Figure 7b). Furthermore, the average
556 simulated daily R rates also indicated low seasonal variability on the plateau compared with
557 the valley. This result is in agreement with the literature, according to which the surface flow
558 rate in the plateau of the study area was low or even absent (Luizão et al, 1989). This is
559 because the higher interception in this area barely reduced the incoming water flux and hence
560 had a minor impact on the R coefficient. The seasonal variability of R rates, which is directly
561 controlled by the seasonal cycle of precipitation, was very well represented by the model,
562 with higher values in the wet season (plateau = 0.4 mm day^{-1} , valley = 2.7 mm day^{-1}) when
563 compared to the dry season (plateau = 0.1 mm day^{-1} , valley = 0.4 mm day^{-1}), in both areas.
564 The INLAND model simulated a peak of R in the valley area during September (0.62 mm
565 day^{-1}), in response to the increase in accumulated mean precipitation in this month (154.9
566 mm), according to observed data (0.43 mm day^{-1}). This happens due to the proximity of the
567 surface water table to the surface in valley area, which may have induced higher soil moisture,
568 generating saturation, and ultimately leading to overland flow. The mean R observed in the
569 valley area was reproduced relatively well by INLAND with strong overestimated during wet
570 season (bias = 1.7) and slight underestimated in the dry season (bias = -0.1) (Table 5). In
571 addition, during the wet season the RMSE was 2.0 mm dia^{-1} and R^2 of 0.72. In the dry season,
572 a reduction in the value of R^2 (0.40) can be observed, indicating a lower correspondence
573 between simulated and observed R data in the valley while RMSE also exhibited a reduction,
574 dropping to 0.2 mm dia^{-1} . The R represented an average value of 3.9% of total precipitation,
575 during 2002 to 2006, in the plateau area. This value is in agreement with other studies in
576 different regions of the Amazon. The average surface runoff estimated at the Ducke Reserve
577 site in the center of the Amazon by Leopoldo et al. (1995) indicated that only 3% of



578 precipitation was directly lost during storm surges through runoff. Germer et al. (2009)
579 identified a surface runoff of only 1% of the precipitation observed in the southwest of the
580 Amazon, while in the Eastern Amazon, Moraes et al. (2006) reported a coefficient of flow of
581 only 2.7%. On the other hand, in valley area the R simulated by INLAND represented a
582 higher part of precipitation when compared to plateau, about 25.3%.

583

584 Deep drainage (D) is also directly linked to precipitation and has a well-defined seasonal
585 cycle, with higher values during the wet season, in both areas, that was very well represented
586 by the INLAND model (Figure 7c). During the wet season, the mean D was 4.3 mm day⁻¹ and
587 2.9 mm day⁻¹ in plateau and valley area, respectively reducing to 0.8 mm day⁻¹ in the plateau
588 and 0.9 mm day⁻¹ in valley area, during the dry season. In addition, the INLAND model
589 simulated a higher D rate in the plateau than in valley area, during the wet season. These
590 differences found between D in both areas occurred because the soil in the plateau is
591 significantly deeper and the water table is located approximately 35 m deep (Tomasella et al.,
592 2008), while in the valley the data showed that the maximum water table depth during the
593 analysis period was approximately 0.6 m. The simulated D in valley area is in accordance
594 with observed data in the same period of 2.4 mm day⁻¹ and 1.6 mm day⁻¹ in wet and dry
595 season, respectively. In general, the INLAND model overestimated R during the wet season
596 (bias 0.5 mm day⁻¹) and underestimated in the dry season (bias = 0.6 mm day⁻¹) (Table 5). The
597 RMSE was 0.7 mm day⁻¹ in both areas and R² of 0.65 indicating a better correspondence
598 between observed and simulated data during the wet season. D values represent a large
599 portion of the total precipitation, corresponding to a mean percentage of 41.3% and 27.2% in
600 plateau and valley area respectively during 2002-2006. Simulated D values simulated on the
601 plateau are in accordance with the value of 40% found by Broedel (2012), in the same study
602 area during 2000-2008. It is however considerably lower than the value of 29.8% reported by
603 Assunção (2011), in the same area.

604

605 Deep drainage added to the runoff results in total runoff (R_{total}). The mean R_{total} simulated
606 during the period from 2002 to 2006 represented 45.2% and 52.5% of the total precipitation,
607 for plateau and shallow area, respectively. The lower percentage of R_{total} in relation to
608 precipitation in the plateau environment is a consequence of a higher ET in this area when
609 compared to the lowland. The mean values of R_{total} in relation to precipitation found in this
610 study, in both areas, showed a good correspondence with the values of 44.3% reported by
611 Tomasella et al. (2008) during the period from 2001 to 2004, and of 49.3% obtained by

612 Broedel (2012) between 2000 and 2008 using the CLM model, the same area of study
 613 (plateau). The value obtained by Broedel (2012) is identical to the value found by Assunção
 614 (2011) in the calibration of the IBIS model. In addition, our results also corroborate with the
 615 value obtained by Cuartas et al. (2012) from 2002 to 2004. Using the DHSVM model, Cuartas
 616 and colleagues reported that the R_{total} value represented 47.5% of the total precipitation in
 617 our study area (plateau).

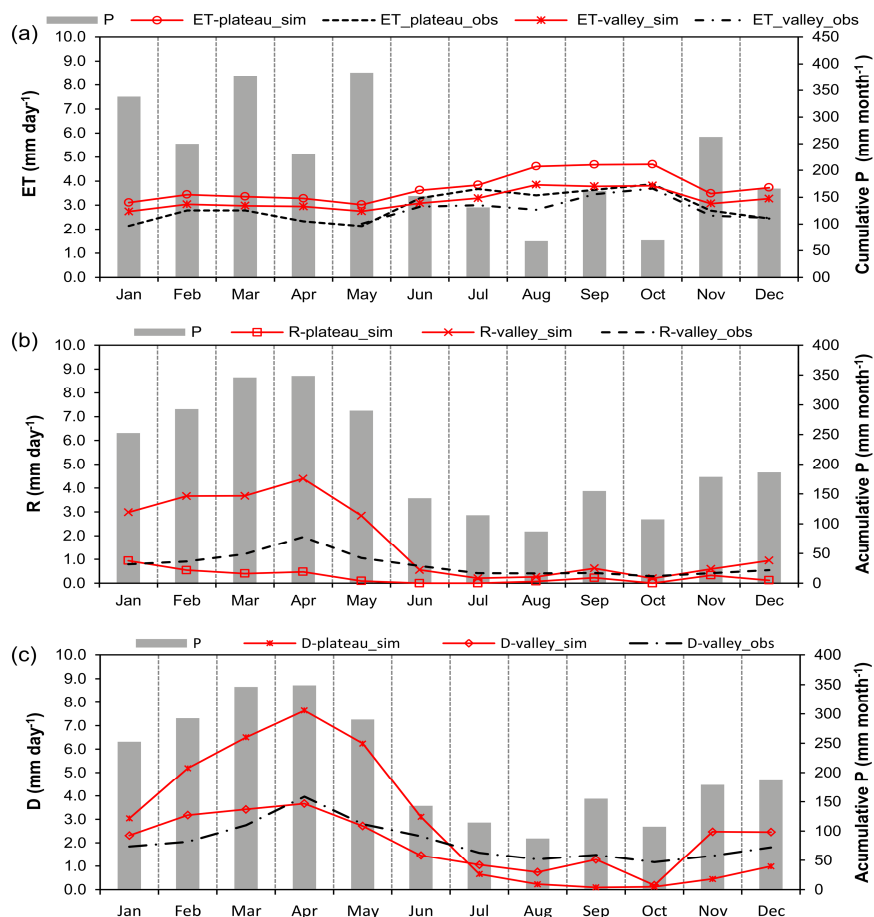
618

619 **Table 5.** Performance of the INLAND model for the representation of the total evaporation (ET) during 2006; R
 620 and D during 2002-2006 located in the study area, from hourly data.

	Flux	Período	Wet season			Dry season		
			RMSE (mm day ⁻¹)	Bias (mm day ⁻¹)	R ² -	RMSE (mm day ⁻¹)	Bias (mm day ⁻¹)	R ² -
Plateau	ET	2006	1,1	0,9	0,71	1,0	0,7	0,64
Valley	ET	2006	1,1	0,2	0,63	0,8	0,4	0,56
	R	2002-2006	2,0	1,7	0,72	0,2	-0.1	0,40
	D	2002-2006	0,7	0,5	0,65	0,7	-0.6	0,64

621

622



623

624 **Figure 7.** Monthly total observed precipitation (bars), observed ET (continuous lines) and simulated total
 625 evaporation, surface runoff and groundwater drainage for the forest canopy (dotted lines).

626

627 *d. Net Ecosystem Exchange for the plateau and valley*

628

629 In general, the simulated daytime and nighttime NEE fluxes suggest that the patterns and
 630 magnitudes were in agreement with observations on the plateau and in the valley in both the
 631 wet and dry seasons. The difference between the two areas was well captured by INLAND
 632 using an unconfined aquifer model to simulated the valley area and corrected vegetation and
 633 soil parameters in both areas (Figure 8 a, b). During the daytime (dominated by
 634 photosynthesis processes), the simulated NEE fluxes on the plateau were slightly higher than
 635 in the valley during the wet and dry seasons, in agreement with observed data. The average



636 NEE flux simulated during the daytime on the plateau, for example, was $-8.5 \mu\text{mol m}^{-2} \text{s}^{-1}$ and
637 $-10.2 \mu\text{mol m}^{-2} \text{s}^{-1}$ in the wet and dry seasons, respectively, whereas in the valley, it decreased
638 to approximately 11.8% and 23.5% of the values in the plateau, during the wet and dry
639 seasons, respectively (Table 6). In contrast, the observed NEE in the plateau presented a
640 mean of $-9.1 \mu\text{mol m}^{-2} \text{s}^{-1}$ and $-8.8 \mu\text{mol m}^{-2} \text{s}^{-1}$ in the wet and dry season, respectively, while
641 in valley the NEE fluxes showed a decrease of 25.3% fall in the wet season and 30.7% in the
642 dry season. The observed values are in agreement with Malhi et al. (1998) of $10.2 \mu\text{mol m}^{-2} \text{s}^{-1}$
643 ¹ measured in central Amazonia using eddy covariance, close to study site,. According to
644 Castilho et al. (2006) the higher NEE rate during the daytime on the plateau is suggestive of a
645 stronger CO_2 uptake rate due to more photosynthetic activity resulting from the higher
646 biomass found in this area. According to Laurance et al. (1999), the biomass variation
647 between plateau and valley is mainly associated with nitrogen availability in both areas. The
648 plateau area has a greater amount of nitrogen both in the soil and in the leaves of the plants
649 when compared to the valley, which indicates a greater amount of available resources for the
650 growth of the plants in this area (Luizão et al. 2004). Luizão (1989) conducted a three year
651 long litterfall experiment in an area 10 kilometers to the northwest of study site and showed
652 that on the plateau a 3 year mean of $8.3 \text{ tons C ha}^{-1}$ of litter was produced, with only 7.4 tons
653 C ha^{-1} in the valley, indicating that plateau area has higher productivity than the valley. In
654 addition, using sapflow data from Zanchi (2013) for the study site, Stijnman (2015) showed
655 that photosynthesis starts later and ends earlier in the valley area. According to Stijnman
656 (2015), the start and end of sapflow in our study site is linking with solar radiation.

657

658 The observed NEE fluxes during daytime did not indicate a pronounced seasonality. In the
659 plateau area for example, the NEE was only 3.3% and 10.2% higher during the wet season in
660 the plateau and valley, respectively. The simulated data show higher mean values of NEE in
661 the dry season, probably due to a higher solar radiation during this period, mainly in the
662 plateau area (20%). Similar behavior was found by Asunção (2011), through the calibration of
663 the IBIS model for the same area of study. The observed daytime NEE values, using eddy
664 covariance, in several areas of Amazonia indicated diverging trends between wet and dry
665 season. The results found by Goulden et al. (2004), for example, in the east of Amazonia
666 indicate higher forest assimilation during the dry season. However, according to Goulden et
667 al. (2004), these results are opposite to those expected, based on forest biomass increment
668 observations, which showed a clear increase during the wet season. In central Amazonia, the
669 data from Malhi et al. (1998) showed higher values in the wet season, related with the rainfall,



670 in agreement with observed data from our study site. Despite this, the INLAND model did not
671 represent well the mean seasonality over 2006, but there was a good agreement with the
672 observed daily peak. In the plateau, for example, the maximum values found between 11:00
673 and 12:00 hours were $-20.3 \mu\text{mol m}^{-2} \text{s}^{-1}$ and $-16.7 \mu\text{mol m}^{-2} \text{s}^{-1}$ and in the dry and wet season,
674 respectively. These values are close to the observed data in the plateau area, whose peaks
675 occurred between 10:00 and 11:00, $-21.9 \mu\text{mol m}^{-2} \text{s}^{-1}$ in the dry season and $-21.5 \mu\text{mol m}^{-2} \text{s}^{-1}$
676 in the wet season. In the valley area, small values of $-15.3 \mu\text{mol m}^{-2} \text{s}^{-1}$ and $-14.3 \mu\text{mol m}^{-2} \text{s}^{-1}$
677 were found in the dry and wet season, respectively (between 11: 00-12: 00), values
678 comparable to those observed of $-19.9 \mu\text{mol m}^{-2} \text{s}^{-1}$ in the dry season (at 11:00) and $-17 \mu\text{mol}$
679 $\text{m}^{-2} \text{s}^{-1}$ in the wet season (at 10:00).

680

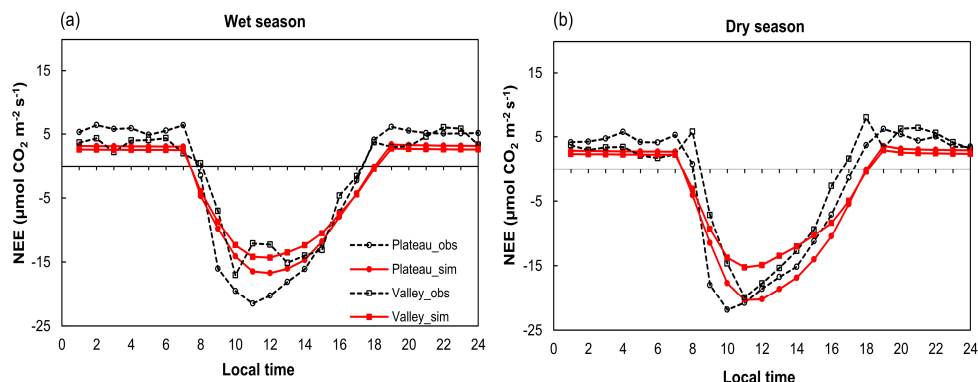
681 The INLAND model simulated very well the mean NEE fluxes during the night (dominated
682 by respiration processes), showing higher values on the plateau area in both seasons. The
683 mean of $3.2 \mu\text{mol m}^{-2} \text{s}^{-1}$ and $2.9 \mu\text{mol m}^{-2} \text{s}^{-1}$ was found in the wet and dry season,
684 respectively, while in the valley the data indicate a reduction of 18.8% in the wet season and
685 17.2% in the dry season, values that show good correspondence with observed data of 24%
686 and 13.3% in wet and dry seasons, respectively (Table 6). According to Araújo (2009), there
687 are two possible explanations for this difference. First, due to either dynamically unstable and
688 turbulent flow or neutral atmosphere above the canopy on the plateau (in contrast to
689 dynamically stable and laminar flow above the canopy in the valley), a more efficient vertical
690 transport is favored. Second, the CO_2 stoke fluxes decreased throughout the night in the
691 valley, whereas this was not the case on the plateau. In addition, the lower values of
692 respiration in the fallow, in both seasons, may also be associated with a lower decomposition
693 rate of organic matter in this area. According to Luizão et al. (2004), the canopy of the
694 vegetation in the valley area have lower values of C:N ratio, which confers poor quality to the
695 leaves of the plants and consequently leads to a reduction of the decomposition process. The
696 INLAND model also simulated satisfactorily the seasonality of observed NEE fluxes during
697 the night, which was slightly higher during the wet season, suggesting a higher respiration
698 rate of the plants for the forest during the months with higher precipitation. This increase
699 corresponded to 10.3% and 8.3% in the plateau and valley, respectively, values comparable to
700 observed data, of 20% in the plateau and 5.1% in the valley. In part, this can be explained by
701 increasing of the air humidity that favors an intense organic matter decomposition by the
702 decomposing microorganisms (Luizão and Schubart, 1987). In contrast to the wet season,
703 during the dry season higher temperatures and greater moisture limitation favors the limitation



704 of microbial activity (Malhi et al., 1998), mainly in plateau area. The proximity of the water
705 table depth to the surface in the valley area ensures a humid environment for a good part of
706 the year, even during the dry season. In addition, during the wet season a greater cloudiness
707 and amount of water vapor is observed in the atmosphere, contributing to a lower loss of
708 longwave radiation (Lin) and less cooling of the vegetation canopy. This influences the
709 stability of the atmosphere, which becomes dynamically unstable and consequently favors
710 vertical transport and mixing of CO₂ fluxes by the forest, both in the plateau and valley areas,
711 during the wet season (Araújo, 2009; Miller et al., 2004). Other studies also found higher
712 respiration values during the wet season. Zanchi et al. (2014) found higher soil respiration or
713 R_{soil} (microbial and fungal together with plant roots) during the wet season in the study site,
714 for both plateau and valley area. Higher values of R_{soil} also was found by Souza (2004) in the
715 plateau area, in the same study site.

716

717 In general, all observed NEE fluxes were underestimated by model, mainly during the dry
718 season in the valley area (Table 6). This underestimation, also found by Assunção (2011) in
719 the same study area, is due to the overestimated NEE value obtained by the eddy covariance
720 method, observed since the first tests performed using this methodology (Ontaki, 1984). The
721 eddy covariance method underestimates the flux of CO₂ under stable atmospheric conditions
722 during the night (Miller et al., 2004), when CO₂ flow is characterized by autotrophic
723 respiration and the decomposition of organic material from soil. The drainage of CO₂ from
724 the highest areas, as is the case of the site of tower K34, to the lower parts, located in the
725 bottom of the valley (Tóta et al. 2008; Araújo et al. 2010) also contributes to the
726 underestimation of forest CO₂ flow at night. In addition, the lowest values of R² also were
727 founding in the valley area (Table 6), suggesting a lower agreement between the observed and
728 simulated NEE values, especially during the dry season (0.55) when compared to the wet
729 season (0.63). The R² values in the plateau (wet = 0.76; dry = 0.66) are higher than those
730 found by Assunção (2011) and Imbuzeiro (2005) of 0.54 and 0.41, respectively, both in the
731 same study area. On the other hand, the RMSE values of the two areas were very similar. In
732 the plateau, for example, it was 6.6 μmol m⁻² s⁻¹ and 7.2 μmol m⁻² s⁻¹ in the wet and dry
733 season, respectively, while in the valley, corresponding values were 6.4 in the season and 7.5
734 in the dry season. These values are close in magnitude to that reported by Imbuzeiro (2005),
735 of 4.2 μmol m⁻² s⁻¹, in the plateau area.



736
 737 **Figure 8.** Average daily observed and modeled net ecosystem exchange (NEE) rates between the ecosystem and
 738 the atmosphere). During the daytime, negative values represent the uptake of CO₂ from the atmosphere
 739 (photosynthetic activity is higher than respiration), whereas a positive flux at nighttime is associated with
 740 emissions of CO₂ from the forest to the atmosphere (respiration activity only).

741

742 **Table 6.** Average observed and simulated net ecosystem exchange (NEE) values for the plateau and valley
 743 during the day (06:00–18:00 h), night (18:00–06:00 h) and daily totals. The Daily peak observed and simulated
 744 as also includes.

	Wet season				Dry season			
	$\mu\text{mol CO}_2 \text{ m}^{-2} \text{ s}^{-1}$				$\mu\text{mol CO}_2 \text{ m}^{-2} \text{ s}^{-1}$			
	Daytime	Nighttime	Daytime peak	Daily total	Daytime	Nighttime	Daytime peak	Daily total
Plateau-Obs	-9.1	5.4	-21.5	-2.4	-8.8	4.5	-21.9	-2.8
Plateau-Sim	-8.5	3.2	-16.7	-3.2	-10.2	2.9	-20.3	-4.2
Valley-Obs	-6.8	4.1	-15.1	-1.8	-6.1	3.9	-19.9	-1.5
Valley-Sim	-7.5	2.6	-14.3	-2.9	-7.8	2.4	-15.3	-3.1

745

746 **Table 7.** Performance of the INLAND model for the representation of the net ecosystem exchange (NEE) during
 747 2006, from hourly data.

	Plateau		Valley	
	Wet season	Dry season	Wet season	Dry season
RMSE ($\mu\text{mol CO}_2 \text{ m}^{-2} \text{ s}^{-1}$)	6.6	7.2	6.4	7.5
Bias ($\mu\text{mol CO}_2 \text{ m}^{-2} \text{ s}^{-1}$)	-0.7	-1.5	-0.8	-1.7
R ² (dimensionless)	0.76	0.66	0.63	0.55

748

749 *e. Energy fluxes for the plateau and valley*

750



751 The simulated Rn diurnal evolution was very similar over the plateau and valley during the
752 wet and dry seasons, which was mainly due to incoming solar radiation and because both
753 have the same meteorological characteristics (Figure 10 a, b). The R^2 of the plateau was 0.99
754 in both the wet (RMSE of 11.7 W m^{-2}) and dry (RMSE of 11.3 W m^{-2}) seasons, whereas for
755 the valley, it was 0.99 in the dry season (RMSE of 29.8 W m^{-2}) and 0.97 (RMSE 44.7 W m^{-2})
756 in the wet season (Table 8). In general, the simulated Rn was slightly underestimated in the
757 valley. One possible explanation for this difference is that the simulated albedo in both the
758 wet and dry seasons was higher than the observed values. The constant albedo simulated by
759 INLAND in the valley were 10.5% and 10.8% in the wet and dry seasons, respectively. These
760 values are 5% (wet season) and 3% (dry season) higher than previous observational values
761 (Araújo, 2008; Oliveira, 2010). Furthermore, this difference could be due to reduced
762 incoming longwave radiation, which is derived from meteorological data input in the model in
763 the plateau. According to Araújo (2008), observed incoming longwave radiation is
764 consistently higher in the valley than on the plateau. The INLAND model simulated very well
765 the difference of the albedos in both areas, showing higher values on the plateau (wet season
766 = 12%; dry season = 12.3%) in agreement with observed data (wet season = 11%; dry season
767 = 12%) from Araújo (2008) and Oliveira (2010). The correct adjustment of albedo in both
768 areas was made through reflectance of near infrared radiation from leaves, i.e.,
769 *rhoevg_NIR* parameter of the 0.31 and 0.26 to plateau and valley respectively (Table 1).
770 According to Leitão (1994), this difference between both areas is caused by the vegetation
771 canopy structure. In the valley area, the foliage of the vegetation grouped in the canopy
772 exhibits larger peaks and depressions organized on the canopy surfaces, and a large amount of
773 incident solar radiation penetrates the canopy before being reflected (Shuttleworth, 1989). In
774 contrast, the vegetation in plateau area is denser which favors a greater homogeneity of the
775 vegetation, resulting in a greater reflectivity of the solar radiation. The seasonality of albedo
776 also was very well representing by INLAND, with higher values during dry season.
777 According to Malhi et al. (1998) the canopy of the forest is darker during the rainy season,
778 due to the seasonality of the precipitation, favoring greater absorption of radiation and
779 consequently lower albedo.

780

781 The model was able to accurately simulate the partitioning of available energy (Rn) with
782 higher percentage of Rn destined for LE flux, followed by H flux, also verified by Araújo et
783 al. (2002), Malhi et al. (2002) and Randow et al. (2004). This was possible especially using the
784 vegetation and soil parameters modified for each area (Table 1) and water table dynamic in



785 the valley area. For the plateau, the LE and H annual averages corresponded to 84.9%, 14.8%
786 of R_n , respectively while the corresponding values in the valley were 72.9% and 26.5%.
787 These values were found to agree well with the observations, of 60.4% (LE) and 21.3% (H)
788 for the plateau and 50% (LE) and 21.9% (H) for the valley. The simulated LE was higher on
789 the plateau than in the valley, particularly in the dry season (Figure 10 c, d) according to
790 observed data. One possible explanation for this difference is the higher LAI on the plateau,
791 which produced a higher evapotranspiration rate. According to Marques-Filho et al. (2005),
792 the LAI on the plateau is $6.1 \text{ m}^2 \text{ m}^{-2}$, whereas in the valley, the value may be approximately
793 13% smaller (Zanchi et al., 2014). Another possible reason is the excess water in the valley
794 soils, which can produce oxygen-deficient roots and affect plant survival and functioning
795 (Pezeshki and DeLaune, 2012). The simulated LAI for the mentioned period was
796 approximately $6.1 \text{ m}^2 \text{ m}^{-2}$ on the plateau and $5.8 \text{ m}^2 \text{ m}^{-2}$ in the valley. These values were
797 found to agree well with Cuartas et al (2012) for the same study area during the period from
798 2002 to 2006. The INLAND model overestimated the LE flux on the plateau and in the
799 valley. The overestimation was stronger on the plateau, where we found an RMSE of 63.8 W m^{-2}
800 and R^2 of 0.85 in the wet season and an RMSE of 66.8 W m^{-2} and R^2 of 0.88 in the dry
801 season. In the valley, the RMSE and R^2 were 63.6 W m^{-2} and 0.72 in the wet season,
802 respectively, whereas in the dry season, the RMSE were slightly smaller, i.e., approximately
803 59.6 W m^{-2} with a R^2 of 0.81, respectively (Table 8). The most likely reason for the
804 overestimation of the simulated LE is the large hourly errors caused by underestimation of the
805 observational LE, which led to the unclosed energy balance. The INLAND model also
806 simulated very well the seasonality of LE, showing higher values during dry season in both
807 areas (plateau = 124.6 W m^{-2} ; valley = 103.6 W m^{-2}) when compared to wet season (plateau =
808 97.2 W m^{-2} ; valley = 86.3 W m^{-2}) which can also be clearly visualized in the observed data.

809

810 In contrast to LE fluxes simulated by INLAND, the simulated H fluxes are higher in the
811 valley area when compared to the plateau, in both wet (valley = 29.8 W m^{-2} ; plateau = 18.6 W m^{-2})
812 and dry (valley = 39.8 W m^{-2} ; plateau = 19.5 W m^{-2}) seasons (Figure 9 e, f). This
813 behavior is in agreement with the observed H fluxes mainly during dry season (valley = 36.7
814 W m^{-2} ; plateau = 33.6 W m^{-2}), indicating a good performance of INLAND. The diurnal cycle
815 also reveals that the seasonality of the H flux was very well reproduced by the model,
816 presenting higher values during the dry season in both areas, in perfect agreement with the
817 observed data. This strong seasonality in H data occurs because, during the dry season, a
818 higher value of incident solar radiation (S_{in}) is recorded in Amazonia, due to the lower

819 cloudiness in the region (Araújo, 2009). The mean values of incident radiation found by
820 Araújo (2009) in the valley area, were 44.6% higher in the dry season of 2006. The higher
821 values of H in the valley, compared to the plateau, suggest that more Rn was used for the H
822 flux in the valley area during the dry months (consequently less energy for the LE flow). This
823 finding may be due to the smaller aboveground live biomass in the central Amazon forests
824 that grows in bottomland areas such as valleys (Laurence et al., 1999; Castilho et al. 2006).
825 This scenario appears to be the case in our study area, where bigger trees tend to occur more
826 frequently on high and flat areas that are dominated by clay soils (Ranzani, 1980; Oliveira and
827 Amaral, 2004), whereas they are sparser in the bottom of the valley (Nobre, 1989). Figure 9
828 (e, f) also shows the significant bias in the simulated values of H for the valley; the model
829 overestimated the observed hourly totals by 11% and 2% during the dry ($R^2 = 0.78$; RMSE =
830 34.9 W m^{-2}) and wet ($R^2 = 0.66$; RMSE = 34.3 W m^{-2}) seasons, respectively. This
831 overestimation in the H flux was related to one of the most relevant parameters for the
832 simulation of H, *rhoevveg_NIR* (Varejão et al. 2011). The sensible heat flux from vegetation to
833 the air is a function of the leaf and stem temperatures and these two variables are dependent
834 on the solar radiation absorbed by the canopies and soil as well as on the net absorbed fluxes
835 of infrared radiation.

836

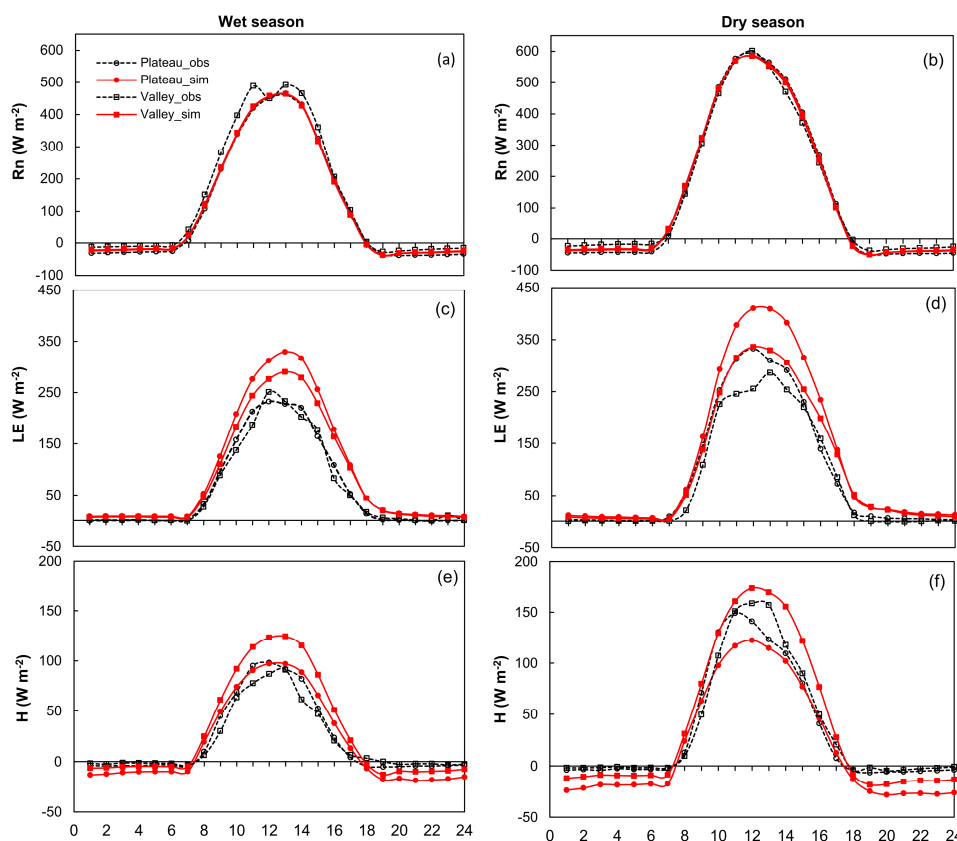
837

838 **Table 8.** RMSE, bias and R^2 calculated for the hourly energy and NEE fluxes.

		Wet season			Dry season		
		RMSE	Bias	R^2	RMSE	Bias	R^2
		(W m^{-2})	(W m^{-2})	-	(W m^{-2})	(W m^{-2})	-
Plateau	Rn	11.7	-4.3	0.99	11.3	-2.2	0.99
	LE	63.8	-34.0	0.85	66.8	-32.6	0.88
	H	26.4	2.8	0.75	33.4	14.2	0.78
Valley	Rn	44.7	15.0	0.97	29.8	10.8	0.99
	LE	63.6	-16.5	0.72	59.6	-20.8	0.81
	H	34.3	-11.0	0.66	34.9	-2.0	0.78

839

840



841

842

Figure 9. Observed and modeled energy fluxes on an hourly basis in the wet and dry seasons of 2006.

843

844

g. Biomass and productivity of vegetation on the plateau and in the valley

845

The results of the analysis suggest that the INLAND model reasonably reproduced the biomass (leaves, wood and root) and carbon flux variability over the plateau and valley (Table 9). The biomass stocks and carbon fluxes on the plateau were greater than in the valley over the 100 years of simulation. The aboveground biomass stock (leaves and wood) on the plateau in the *DVI* simulation was 172.6 tons C ha⁻¹, whereas in the valley, it was approximately 124.3 ton C ha⁻¹. The aboveground biomass stocks in the second simulation set, *DV2*, showed a reduction of 28% on the plateau and 38% in the valley. This finding is not surprising because the *DVI* simulation had more initial biomass than *DV2*. The aboveground biomass simulated by INLAND on the plateau and in the valley was similar to the value obtained by Higuchi et al. (2016), i.e., 188 tons C ha⁻¹ in an area of 3 ha of forest located near our site. The value identified by Malhi et al. (2006) in the same region (10 ha) was 148 tons C ha⁻¹.

855



856 According to Malhi et al. (2006), the aboveground biomass in the eastern Amazon is
857 equivalent to 150-175 tons C ha⁻¹. Our simulations agree with the stock value of 167 tons C
858 ha⁻¹ estimated by Pyle et al. (2008) for the central Amazon for 20 ha of forest, same value of
859 estimative from Johnson (2016) to central Amazonia. In all of these studies, the aboveground
860 biomass was considered as the mean of the entire transect that encompasses a plateau-valley
861 mosaic. The differences in aboveground biomass between the plateau and valley is in
862 agreement with several studies in the region (Castilho et al. 2006; Zarin et. al 2001, Laurence
863 et al 2001; Luizão et al. 2004) indicating good performance of INLAND. Some of these
864 differences are due to the forest structure, as plateau areas have a greater proportion of large
865 trees than valley bottoms (Malhi et al., 2009b). Furthermore, the biomass is influenced by
866 soils, and more fertile soils tend to favor fast-growing plants and low wood density (Malhi et
867 al. 2004), which allocates more energy to wood and leaf production and less to structural and
868 chemical defenses and their associated metabolic costs (Malhi et al. 2009b). Castilho et al.
869 (2006), for example, found that tree biomass tended to increase in clay-rich soils (located in
870 plateaus), whereas sandier soils (located in valleys) are characterized by lower productivity
871 (Zarin et al. 2001). Laurance et al. (1999) attributed the great spatial variation on aboveground
872 biomass estimates to nitrogen availability. The clayey soils located on high plateau areas are
873 considered more fertile and are characterized by higher nitrogen availability and
874 decomposition rates (Luizão et al. 1989), which provide greater productivity to the forest,
875 indicating that higher carbon fluxes can be found on plateaus and decline toward valley
876 bottoms.

877

878 Coarse and fine roots of live trees compose the belowground biomass stocks. However, the
879 belowground biomass simulated by INLAND is defined only by the fine rootstock, which
880 includes root material less than a threshold diameter, usually 2 mm. According to Malhi et al.
881 (2009 b) the fine roots are a very minor component of the belowground biomass stock, about
882 9.5% of aboveground biomass. The simulated values for both *DVI* and *DV2* were higher on
883 the plateau compared with the valley. The fine root biomass simulated in *DVI* was 1.9 tons C
884 ha⁻¹ and 1.6 ton C ha⁻¹ on the plateau and in the valley, respectively. The *DVI* simulation
885 represented a large reduction of 26% on the plateau and even stronger in the valley,
886 approximately 37%. In general, the model correctly simulated the variability of the fine root
887 biomass over the plateau and valley, with higher values on the plateau. Root biomass would
888 be expected to be low in soils limited by anoxia associated with seasonally higher water
889 tables, such as those found in the valley (Malhi et al., 2009b). However, the simulated results



890 in both environments were underestimated when compared with those of other studies in the
891 central and eastern Amazon, which were realized along a topographic profile in 1 meter of
892 soil. Malhi et al. (2009b) estimated a value of 42 tons C ha⁻¹ belowground biomass (coarse
893 and fine roots) in a forest in the central Amazon, whereas in the east, this value ranged from
894 35 to 48 tons C ha⁻¹. In all these studies, the fine roots showed values of 4 tons C ha⁻¹. A study
895 by Metcalfe et al. (2007) in the same area to the east of the basin reported much lower values
896 of approximately 2 tons C ha⁻¹. The values of belowground biomass in similar forests located
897 within 100 km of one another can exhibit significant differences, and it is not clear what
898 results in these differences (Chambers et al. 2001b).

899

900 The INLAND model simulates both autotrophic (Ra) and heterotrophic (Rh) respiration terms
901 that together represent the total ecosystem respiration (Reco). The simulated values of Rh
902 (CO₂ respired by herbivores, detritivores, and higher trophic levels as they consume and break
903 down organic matter) and Ra (CO₂ directly respired by plants - leaf, wood and root live- as a
904 breakdown product from their own metabolic activity) rates were not significantly different
905 between the *DVI* and *DV2* simulations. The Ra flux for *DVI* simulations varied from
906 approximately 24.9 tons C ha⁻¹ yr⁻¹ to 20.1 tons C ha⁻¹ yr⁻¹ on the plateau and in the valley,
907 respectively. These results are similar to the estimates reported by Malhi et al. (2009b) and
908 Chambers et al. (2004) in the same region (mean of the entire transect) of approximately 19.8
909 tons C ha⁻¹ yr⁻¹ and 21 tons C ha⁻¹ yr⁻¹, respectively. These values also are close to estimates of
910 21.4 tons C ha⁻¹ yr⁻¹ by Malhi et al (2009) in eastern Amazonia. Joetzjer et al. (2015) found
911 higher values, of 25-32 tons C ha⁻¹ yr⁻¹ in central Amazonia using the land surface model
912 ISBACC (Interaction Soil Biosphere Atmosphere Carbon Cycle), from Noilhan and Mahfouf
913 (1996). Rh was significantly lower than Ra, with values for *VDI* simulations varying from 9.4
914 tons C ha⁻¹ yr⁻¹ on the plateau to 9.1 tons C ha⁻¹ yr⁻¹ in the valley. Estimates of Rh from this
915 study were comparable to those previously reported by Malhi et al. (2009b) of 9.6 tons C ha⁻¹
916 yr⁻¹ and Chambers et al. (2004) of 8.5 tons C ha⁻¹ yr⁻¹.

917

918 The Rh (microbial and fungal) together with Ra (plant roots) composed efflux of carbon
919 dioxide (CO₂) from soil or soil respiration (Rsoil). According to Chambers et al. (2004) there
920 is a strong correlation between Rsoil with soil texture, which varied along the topography.
921 The root respiration, for example, is higher in the plateau (7.4 tons C ha⁻¹ yr⁻¹) when
922 compared to the valley (5.8 tons C ha⁻¹ yr⁻¹) area (Matcalfe et al. 2007). This result is opposite
923 that found by Silver et al. (2005), also in eastern Amazonia (plateau = 3.2 tons C ha⁻¹ yr⁻¹;



924 valley = 5.2 tons C ha⁻¹ yr⁻¹), using a very different methodology. The ratio of root respiration
925 to total R_{soil} may vary from 50 to 60% depending on vegetation type and season (Hanson et
926 al., 2002). Chambers et al. (2004) estimated that root respiration accounted for 45% of R_{soil}
927 in our study area. This value is higher than that found by Silver et al. (2005) in east of Amazon, of
928 24–35%. The values of total R_{soil} reported by Chambers et al (2004) were 14.4 tons C ha⁻¹ yr⁻¹
929 for plateau (clayey soils) and 9.8 tons C ha⁻¹ yr⁻¹ for valley (sandy soils), suggesting a good
930 performance of the INLAND model in representing Rh. This result can be explained by lower
931 decomposition rates in valley locations (Luizão et al, 2004). According to Luizão et al,
932 (2004), besides the annual production of litter in valley (6.6 tons C ha⁻¹ yr⁻¹) is lower than in
933 plateau (8.9 tons C ha⁻¹ yr⁻¹), similar to result found by Luizão and Schubart (1987), the higher
934 C:N ratio in the leaves of plants in valleys indicate low quality, suggesting that their
935 decomposition rates may be lower than on plateaus (also reported by Souza, 2004). In
936 addition, it is clear from the early studies, that higher water contents can inhibit CO₂
937 production in soils (Linn and Doran, 1984; Oberbauer et al., 1992; Sotta et al., 2004;
938 Davidson and Janssens, 2006). Sotta et al. (2004), for example, verified a steep 30% drop of
939 R_{soil} after rainfall when compared with nonrain periods. During the year of 2006 it is
940 possible to notice that the precipitation in the study area was higher, in almost all months,
941 than the climatological mean in Manaus (Figure 5). The total accumulated precipitation during
942 this period was 2591 mm, about 20% higher than the climatological mean. Because of the
943 higher precipitation in valley areas, the high phreatic level and exfiltration of groundwater
944 provoked slow diffusion of oxygen into the soil, presumably only allowing for anaerobic
945 decomposition with generally slower degradative enzymatic pathways. The results of R_{soil}
946 from this work are different from those of Zanchi et al (2014) that indicate higher rates on the
947 valley (15.5 tons C ha⁻¹ yr⁻¹) when compared to the plateau (9.8 tons C ha⁻¹ yr⁻¹) area.
948 However, during the period of R_{soil} measurements of Zanchi and co-authors from a plateau
949 area (period completely different than R_{soil} measurements in the valley area), which were
950 undertaken between August 3 until November 6 (2006) and February 21 until February 26
951 (2008), the precipitation was 45.6% and 50.4% higher than the climatological mean in
952 Manaus (Figure 5) indicating a higher replacement of the air filled pores by water that may
953 form a cap and prevent gas diffusion of CO₂ through the soil to the atmosphere.

954

955 One interesting feature to note is the link in INLAND between Rh and NEE or an exchange of
956 carbon as gaseous CO₂ between ecosystems and the atmosphere. The lower value of Rh in the
957 valley can also produce a smaller simulated NEE in this environment. The NEE simulated by



958 INLAND ranged from -0.6 to -0.7 tons C ha⁻¹ yr⁻¹ (for *DV2* and *DVI*, respectively) in the
959 valley, i.e., approximately 40% less than that simulated on the plateau, indicating a lower net
960 CO₂ flux in the forest canopy in the valley forest. However, the NEE simulated by INLAND
961 in both environments are generally very similar to the values found by Malhi et al. (1999) of -
962 1.1 tons C ha⁻¹ yr⁻¹. The NEE was also influenced by changes in the NPP over time, by
963 sequestering atmospheric CO₂, and supplies organic material for Rh. The NPP values
964 simulated in the present study on the plateau, i.e., approximately 10.6 tons C ha⁻¹ yr⁻¹ (*DVI*
965 and *DV2*), were slightly larger than in the valley. The NPP reductions in the valley
966 represented 7% and 8% for *DVI* and *DV2*, respectively, and were similar to the estimate
967 provided by Malhi et al. (2009b) for the central Amazon using flux tower data (10.1 tons C
968 ha⁻¹ yr⁻¹). Furthermore, the simulated NPP was also comparable to the observed average of 9.0
969 tons C ha⁻¹ yr⁻¹ from a forest in the same study region (Malhi et al. 2009b). According to
970 Aragão et al. (2009), the total NPP tends to increase with soil phosphorus (P) and leaf
971 nitrogen (N) status. It is well known from Ferraz et al. (1998) and Luizão et al (2004) that
972 both soil P and leaf N is higher in plateau areas, where the soil has higher clay content.
973 Simulating the NPP together with the GPP in forest biomes is fundamental for realistic global
974 and regional carbon budgets and for projecting how these fluxes are affected by a changing
975 climate (Zha et al. 2013). As expected, the GPP in the plateau was higher than in the valley
976 and area, without significant difference between both *VDI* and *VD2*. The GPPs on the plateau
977 and valley were 36 tons C ha⁻¹ yr⁻¹ and 30 tons C ha⁻¹ yr⁻¹, respectively, agreeing with the
978 estimate of 30.4 tons C ha⁻¹ yr⁻¹ provided by Malhi et al. (1998) close to study site. Similar
979 values were also reported by Malhi et al (2009b) for the same study area, of 29.9 tons C ha⁻¹
980 yr⁻¹, and by Fischer et al (2007) in a forest located at east of Amazonia, with a mean value of
981 31.2 tons C ha⁻¹ yr⁻¹. All the references given here, included both topographical classes
982 (plateau and valley). This reduction of 16.7% in the simulated GPP in the valley can be
983 related with the difference of the LAI and ET in both areas. Since the valley LAI values are
984 lower than those in the plateau and consequently so is ET, this should reduce the GPP and
985 produce a large difference between the plateau and valley area. In addition, in the valley area
986 the sutured condition of this environment could lead to a lower GPP, due to the impact of this
987 condition in the process of transpiration (Feddes et al.,1978), resulting in lower productivity
988 of the forest in this area.

989

990

991 **Table 9.** Average of the last 10 years of the simulations for the carbon fluxes and biomass on the plateau and in
 992 the valley of: GPP (gross primary productivity), NPP (net primary production), NEE (net ecosystem exchange),
 993 Rh (heterotrophic respiration), Ra (autotrophic respiration), leaf biomass, wood biomass and root biomass. The
 994 *VD1* (dynamic vegetation 1) and *VD2* (dynamic vegetation 2) values correspond to the dynamic vegetation and
 995 dynamic vegetation-cold start simulations, respectively.

Variable	Unit	Plateau		Valley	
		VD1	VD2	VD1	VD2
GPP	ton ha ⁻¹ yr ⁻¹	35.5	35.4	29.9	29.9
NPP	ton ha ⁻¹ yr ⁻¹	10.6	10.6	9.9	9.8
NEE	ton ha ⁻¹ yr ⁻¹	-1.2	-1.0	-0.7	-0.6
Ra	ton ha ⁻¹ yr ⁻¹	24.9	24.8	20.1	20.0
Rh	ton ha ⁻¹ yr ⁻¹	9.4	9.5	9.1	9.2
Leaf biomass	ton ha ⁻¹	2.9	2.2	2.4	1.5
Wood biomass	ton ha ⁻¹	169.7	122.5	121.9	75.8
Root fine biomass	ton ha ⁻¹	1.9	1.4	1.6	1.0

996

997

998 4. Conclusions

999 In this study, we demonstrate that the INLAND model is able to reproduce the particularities
 1000 of the observed energy, water and carbon fluxes with reasonable accuracy between two very
 1001 different environments, plateau and valley bottom, in a central Amazonian forest, confirming
 1002 our initial hypothesis. To better represent their characteristics, an adjustment of vegetation and
 1003 soil parameters and the development of a lumped unconfined aquifer model was required to
 1004 account for the water table dynamics in the valley area. The model reasonably reproduces
 1005 ($R^2=0.69$) the observed temporal variability of the water table depth in the valley, including
 1006 its seasonal cycle and interannual differences, in accordance with precipitation variability. On
 1007 the plateau, the mean ET was 13% higher than in the valley, with maximum amplitude in
 1008 August, when the precipitation is lower. The surface runoff is significantly higher in the
 1009 valley bottom during the wet season. The mean surface runoff on the plateau represents a
 1010 small portion (3%) of the total precipitation over the entire period. In the valley, this
 1011 percentage is much larger, representing approximately 25% of total precipitation.

1012

1013 The INLAND model also captured the difference in the partitioning of incoming energy and
 1014 carbon fluxes, mainly LE, H and NEE fluxes in both seasonal and diurnal time scales. On the
 1015 plateau, the simulated LE flux is higher than in the valley during both the wet and dry
 1016 seasons, due to its higher biomass stock, allowing more energy to be used for the LE flux.
 1017 The opposite behavior is observed for the simulated H flux, as in the valley bottom area lower



1018 stock biomass favor less energy used in LE flux and consequently a higher H flux in both
1019 seasons. A large difference between the wet and dry seasons is observed in our results, with
1020 much higher H values during the dry season, when more radiation is incident to the surface.
1021 The seasonal variability also shows that the values of LE are higher during the dry season
1022 than in the wet months, in both areas. In general, NEE is higher on the plateau during both the
1023 wet and dry seasons. During the dry season, when simulated NEE is higher, the reduction in
1024 the valley is 26%, with a value of only 9.2% during the wet season. Our results suggest that
1025 the model also reasonably reproduces the biomass and carbon flux variability between the
1026 plateau and valley. The biomass values show significant differences between the two
1027 environments. In general, the dynamic vegetation module using the aboveground biomass
1028 pool (leaves and wood) is much smaller in the valley than on the plateau after 100 years of
1029 model simulation. The biomass reductions in the valley represent 28% and 38% of the two
1030 sets of simulations, i.e., *DV1* and *DV2*, respectively. The simulation of belowground biomass
1031 does not reproduce well the values observed in other studies in the region. However, all of the
1032 simulated fluxes are higher on the plateau than in the valley, suggesting the larger
1033 productivity of the plateau forest, in agreement with the available studies in the central and
1034 eastern Amazon.

1035

1036

1037 **References**

1038 Alvares, C. A., Stape, J. L., Sentelhas, P. C., Gonçalves, J. L. M., Sparovek, G.: Köppen's
1039 climate classification map for Brazil, *Meteorologische Zeitschrift*, 22(6), 711-728, doi:
1040 10.1127/0941-2948/2013/0507, 2014.

1041

1042 Ambrose, R. B., Roesch, S. E.: Dynamic Estuary Model Performance. *Journal of*
1043 *Environmental Engineering Division*, 108 (1), 51-71, 1982.

1044

1045 Anderson, L. O., Malhi, Y., Ladle, R. J., Aragão, L. E. O. C., Shimabukuro, Y., Phillips, O.
1046 L., Baker, T., Costa, A. C. L., Espejo, J. S., Higuchi, N., Laurance, W. F., Lopez-Gonzalez,
1047 G., Monteagudo, A., Nunez, V. P., Peacock, J., Quesada, C. A., Almeida, S., Vasquez, M. R.:
1048 Influence of landscape heterogeneity on spatial patterns of wood productivity, wood specific
1049 density and above ground biomass in Amazonia. *Biogeosciences*, 6,1883-1902. doi:
1050 10.5194/bg-6-1883-2009, 2009.

1051

1052 Aragão, L. E. O. C., Malhi, Y., Metcalfe, D. B., Silva-Espejo, J. E., Jiménez, E., Navarrete,
1053 D., Almeida, S., Costa, A. C. L., Salinas, N., Phillips, O. L., Anderson, L. O., Alvarez, E.,
1054 Baker, T. R., Goncalvez, P. H., Huamán-Ovalle, J., Mamani-Solórzano, M., Meir, P.,
1055 Monteagudo, A., Patiño, S., Peñuela, M. C., Prieto, A., Quesada, C.A., Rozas-Dávila, A.,
1056 Rudas, A., Silva Jr, J. A., Vásquez, R.: Above and below-ground net primary productivity



- 1057 across ten Amazonian forests on contrasting soils. *Biogeosciences*, 6,2759–2778.
1058 doi:10.5194/bg-6-2759-2009, 2009.
- 1059
- 1060 Araújo, A. C., Kruijt, B., Nobre, A. D., Dolman, A. J., Waterloo, M. J., Moors, E. J., De
1061 Souza, J. S.: Nocturnal accumulation of CO₂ underneath a tropical forest canopy along a
1062 topographical gradient. *Ecological Applications*, 18, 1406-1419, doi: 10.1890/06-0982.1,
1063 2008.
- 1064
- 1065 Araújo, A. C. Spatial variation of CO₂ fluxes and lateral transport in an area of terra firme
1066 forest in Central Amazonia. 2009. 158 p. Tese de doutorado (Doutorado em Ciências
1067 Geoambientais) - Free University of Amsterdam, Holanda.
- 1068
- 1069 Araújo A. C, Nobre A. D, Kruijt B, Elbers J. A, Dallarosa R, Stefani P, Von Randow C,
1070 Manzi A. O, Culf A. D, Gash, J. H. C, Valentini R, Kabat P.: Comparative measurements of
1071 carbon dioxide fluxes from two nearby towers in a central Amazonian rain forest: The
1072 Manaus LBA site. *Journal of Geophysical Research*, 107, 1-20, doi: 10.1029/2001JD000676,
1073 2002.
- 1074
- 1075 Araújo, A. C., Dolman, A. J., Waterloo, M. J., Gash, J. H. C., Kruijt, B., Zanchi, F. B., Lange,
1076 J. M. E., Stoevelaar, R., Manzi, A. O., Nobre, A. D., Lootens, R. N., Backer, J.: The spatial
1077 variability of CO₂ storage and the interpretation of eddy covariance fluxes in central
1078 Amazonia. *Agricultural and Forest Meteorology*, 150, 226-237,
1079 doi:10.1016/j.agrformet.2009.11.005, 2010.
- 1080
- 1081 Arnold, J. G. and Allen, P. M.: Automated methods for estimating baseflow and ground water
1082 recharge from streamflow records. *Journal of the American Water Resources Association*, 35
1083 (2), 411-424. doi: 10.1111/j.1752-1688.1999.tb03599.x, 1999.
- 1084
- 1085 Assunção, L.: Aplicação do modelo de vegetação dinâmica IBIS às condições de floresta
1086 de terra firme na região central da Amazônia. 103 p. Tese de Mestrado (Mestrado em
1087 Clima e Ambiente), Instituto Nacional de Pesquisas da Amazônia/ Universidade do Estado do
1088 Amazonas (INPA/UEA), Manaus, 2011.
- 1089
- 1090 Ayres, J. M. As matas de Várzea do Mamirauá: Médio Rio Solimões. Brasília: MCT-CNPq,
1091 Tefé, 1995.
- 1092
- 1093 Bravard, S. and Righi, D.: Geochemical differences in an Oxisol-Spodosol Toposequence of
1094 Amazonia, Brazil. *Geoderma*, 44, 29-42, doi: 10.1016/0016-7061(89)90004-9, 1989.
- 1095
- 1096 Broedel, E. Estudo da dinâmica de água no solo em uma área de floresta primária não
1097 perturbada na Amazônia Central. 149 p. Tese de Mestrado (Mestrado em Clima e Ambiente),
1098 Instituto Nacional de Pesquisas da Amazônia/ Universidade do Estado do Amazonas
1099 (INPA/UEA), Manaus, 2012.
- 1100
- 1101 Broedel, E., Tomasella, J., Cândido, L. A., Von Randow, C.: Deep soil water dynamics in an
1102 undisturbed primary forest in central Amazonia: differences between normal years and the
1103 2005 drought, *Hydrological Processes*, doi: 10.1002/hyp.11143, 2017.
- 1104
- 1105 Campbell, G. S. and Norman, J. M.: An Introduction to environmental biophysics, 2.ed. New
1106 York: Springer, 286p. <http://dx.doi.org/10.1007/978-1-4612-1626-1>, 1998.



- 1107
1108 Castilho, C. V de., Magnusson, W. E., Araújo, R. N. O de., Luizão, R. C. C., Luizão, F. J.,
1109 Lima, A. P., Higuchi N.: Variation in aboveground tree life biomasses in a central Amazonian
1110 forest: effects of soil and topography, *Forest Ecology and Management*, 234, 85-96,
1111 doi:10.1016/j.foreco.2006.06.024,2006.
1112
1113 Chambers, J. Q., Santos, J., Ribeiro, R. J., Higuchi, N.: Tree damage, allometric relationships,
1114 and above-ground net primary production in central Amazon Forest. *Forest Ecology and*
1115 *Management.*, 152(1-3), 73-84, doi:10.1016/S0378-1127(00)00591-0, 2001b.
1116
1117 Chambers, J. Q., Higuchi, N., Teixeira, L. M., dos Santos, J., Laurence, S. G., Trumbore, S.
1118 E.: Response of tree biomass and wood litter to disturbance in a central amazon forest,
1119 *Oecologia*, 141,596-611, doi: 10.1007/s00442-004-1676-2, 2004.
1120 Chauvel, A., Lucas, Y., Boulet, R.: On the genesis of the soil mantle of the region of Manaus,
1121 central Amazonia. Brazil, *Experientia*, 43: 234-241, 1987.
1122
1123 Clapp, R .B. and Hornberger, G. M.: Empirical equations for some soil hydraulic properties.
1124 *Water Resources Research*, 14(4), 601-604, 1978.
1125
1126 Climanálise, 2003. Boletim de monitoramento e análise climática.Retrieved from:
1127 www.cptec.inpe.br/products/climanalise/ [accessed 20 November 2016].
1128
1129 Cuartas, L. A., Tomasella, J., Nobre, A. D., Hodnett, M. G., Waterloo, M. J., Munera, J. C.:
1130 Interception water-partitioning dynamics for a pristine rainforest in Central Amazonia:
1131 Marked differences between normal and dry years. *Agricultural and Forest Meteorology*, 145,
1132 69-83, doi:10.1016/j.agrformet.2007.04.008, 2007.
1133
1134 Cuartas, L. A., Tomasella, J., Nobre, A. D., Nobre, C. A., Hodnett, M. G., Waterloo, J. M., de
1135 Oliveira, S. M., von Randow, R. C., Trancoso, R., Ferreira, M.: Distributed hydrological
1136 modeling of a micro-scale rainforest watershed in Amazonia: Model evaluation and advances
1137 in calibration using the new HAND terrain model, *Journal of Hydrology*, 462/463, 15-27, doi:
1138 10.1016/j.jhydrol.2011.12.047, 2012.
1139
1140 Da Rocha, H. R., Manzi, A. O., Cabral, O. M., Miller, S. D., Michael, L. G., Saleska, S. R.,
1141 Coupe, N. R., Wofsy, S. C., Borma,L. S., Artaxo, P., Vourlitis, G., Nogueira, J. S., Cardoso,
1142 F. L., Nobre, A. D., Kruijt, B., Freitas, H. C., Von Randow, C., Aguiar, R. G., Maia, J. F.:
1143 Patterns of water and heat flux across a biome gradient from tropical forest to savanna in
1144 Brazil, *Journal of Geophysical Research*, 114: 1-8, doi: 10.1029/2007JG000640, 2009.
1145
1146 Davidson E. A. and Janssens I. A.: Temperature sensitivity of soil carbon decomposition and
1147 feedbacks to climate change. *Nature*, 440:165-173. doi:10.1038/nature04514, 2006.
1148
1149 Drucker D. P.: Modelagem Hidrológica de uma Microbacia em Manaus, AM, Brazil.
1150 Piraçicaba, São Paulo. 24pp, 2001.
1151
1152 Fan, Y. and Miguez-Macho, G.: Potential groundwater contribution to Amazon dry-season
1153 evapotranspiration, *Hydrology and Earth System Sciences*, 14, 2039–2056, doi:10.5194/hess-
1154 14-2039-2010, 2010.
1155



- 1156 Farquhar, G. D., von Caemmerer, S., Berry, J. A.: A biochemical model of photosynthetic
1157 CO₂ assimilation in leaves of C₃ species. *Planta* 149: 78-90. doi: 10.1007/BF00386231,
1158 1980.
- 1159
- 1160 Feddes, R. A., P. J. Kowalik., Zaradny H.: Simulation of Field Water Use and Crop Yield,
1161 Simulation Monographs, PUDOC, Wageningen, The Netherlands, 189 pp, 1978.
- 1162
- 1163 Ferraz, J., Ohta, S., Sales, P. C.: Distribuição dos solos ao longo de dois transectos em
1164 floresta primária ao norte de Manaus (AM). *Pesquisas florestais para a conservação da*
1165 *floresta e reabilitação de áreas degradadas da Amazonia- Manaus. Instituto Nacional de*
1166 *Pesquisas da Amazônia*, 111-143, 1998.
- 1167
- 1168 Ferreira, S. J. F.; Luizão, F. J.; Mello-Ivo, W.; Ross, S. M.; Biot, Y.: Propriedades físicas
1169 do solo após extração seletiva de madeira na Amazônia central, *Acta Amazonica*, 32(3), 449-
1170 466, 2002.
- 1171
- 1172 Ferreira, S. J. F., Luizão, F. J., Dallarosa, R. L .G.: Precipitação interna e interceptação da
1173 chuva em floresta de terra firme submetida a extração seletiva de madeira na Amazônia
1174 Central, *Acta Amazônica*, 35(1), 55-62, doi: 10.1590/S0044-59672005000100009, 2005.
- 1175
- 1176 Foley, J. A., Prentice, I. C., Ramankutty, N., Levis, S., Pollard, D., Sitch, S., Haxeltine, A.:
1177 An integrated biosphere model of land surface processes, terrestrial carbon balance, and
1178 vegetation dynamics, *Global Biogeochemical Cycles*, 10, 603-628, doi: 10.1029/96GB02692,
1179 1996.
- 1180
- 1181 Foley, J. A., Levis, S., Costa M. H., Cramer, W., Pollard D.: Incorporating dynamic
1182 vegetation cover within global climate models. *Ecological Applications*, 10 (6), 1620-1632,
1183 doi: 10.1890/1051-0761(2000)010[1620:IDVCWG]2.0.CO;2, 2000.
- 1184
- 1185 Furey, P. R. and Grupta V. K. A physically based filters for baseflow separation from
1186 streamflow time series, *Water Resources Research*, 37(11), 2709-2722, doi:
1187 10.1029/2001WR000243, 2001.
- 1188
- 1189 Germer, S., Neill, C., Vetter, T., Chaves, J., Krusche, A. V., Elsenbeer, H.: Implications of
1190 long-term land-use change for the hydrology and solute budgets of small catchments in
1191 Amazonia. *Journal of Hydrology* 364 (3-4):349-363 doi:10.1016/j.jhydrol.2008.11.013, 2009.
- 1192
- 1193 Goulden, M. L., Miller, S. D., da Rocha, H. R., Menton, M. C., de Freitas, H. C., Figueira, A.
1194 M. E. S., de Souza, C.A.D.: Diel and seasonal patterns of tropical forest CO₂ exchange,
1195 *Ecological Applications*, 14 (4), S42-S54, 2004.
- 1196
- 1197 Green, W. H. and Ampt, G.: Studies on soil physics. The flow of air and water through soils.
1198 *The Journal of Agricultural Science*, 4, 1-24, doi:10.1017/S0021859600001441, 1911.
- 1199
- 1200 Hess, L .L., Melack, J. M., Novo, E. M., Barbosa, C., Gastil, M.: Dual-season mapping of
1201 wetland inundation and vegetation for the central Amazon basin, *Remote Sensing of*
1202 *Environment*, 87, 404-428, doi:10.1016/j.rse.2003.04.001, 2003.
- 1203
- 1204 Higuchi, N., Suwa, R., Higuchi, F. G., Lima, A. J. N., dos Santos, J., Noguchi, H., Kajimoto,
1205 T.,



- 1206 Ishizuka, M.: Overview of Forest Carbon Stocks Study in Amazonas State, Brazil. In Nagy L,
1207 Forsberg BR, Artaxo P.(Eds.), Interactions Between Biosphere, Atmosphere and Human
1208 Land Use in the Amazon Basin (Vol. 227) (pp.171-187). Ecological Studies, 2016.
1209
- 1210 Hodnett, M. G., Vendrame, I., Marques-Filho, O. A., Oyama, M .D., Tomasella, J.: Soil
1211 water storage and groundwater behavior in a catenary sequence beneath forest in central
1212 Amazonia. Comparisons between plateau, slope and valley floor. *Hydrology and Earth
1213 System Sciences*, 1, 265-277, doi:10.5194/hess-1-265-1997, 1997a.
1214
- 1215 Hodnett, M. G., Vendrame, I., Oyama, M. D., MArques-Filho, A. O., Tomasella J.: Soil
1216 water storage and groundwater behaviour in a catenary sequence beneath forest in central
1217 Amazonia. Floodplain water table behaviour and implications for stream flow generation,
1218 *Hydrology and Earth System Sciences*, 1, 279-290, doi:10.5194/hess-1-279-1997, 1997b.
1219
- 1220 Hodnett, M. G. and Tomasella, J.: Marked differences between van Genuchten soil water-
1221 retention parameters for temperate and tropical soils: A new water-retention pedotransfer
1222 function developed for tropical soils, *Geoderma*, 108, 155-180, 2002.
1223
- 1224 Imbuzeiro, H. M. A.: Calibração do modelo IBIS na floresta amazônica usando múltiplos
1225 sítios. Dissertação (Mestrado em Meteorologia Agrícola) – Universidade Federal de Viçosa,
1226 Viçosa, Minas Gerais, 92 pp, 2005.
1227
- 1228 Jackson, R. B., Canadell, J., Ehleringer, J. R., Mooney, H. A., Sala, O. E., Schulze, E. D.: A
1229 global analysis of root distributions for terrestrial biomes, *Oecologia*, 108, 389-411, doi:
1230 10.1007/BF00333714, 1996.
1231
- 1232 Joetzjer, E., Delire, C., Douville, H., Ciais, P., Decharme, B., Carrer, D., Verbeeck, H., De
1233 Weirdt, M., and Bonal, D.: Improving the ISBACC land surface model simulation of water
1234 and carbon fluxes and stocks over the Amazon forest, *Geoscientific Model Development*, 8,
1235 1709–1727, doi:10.5194/gmd-8-1709-2015, 2015.
1236
- 1237 Johnson, A.I.: Specific yield compilation of specific yields for various materials. U.S.
1238 Geological Survey., *Water Supply Papers*, 1662-D, 74 pp, 1967.
1239
- 1240 Johnson, M., Galbratith, D., Gloor, M., De Deurwaerder, H., Guimberteau, M., Ramming, A.,
1241 Thonicke, K., Verbeeck, Hans., von Randow, C., et al. 2016. Variation in stem mortality rates
1242 determines patterns of above-ground biomass in Amazonian forests: implications for dynamic
1243 global vegetation models, *Global Change Biology*, doi: 10.1111/gcb.13315, 2016.
1244
- 1245 Kucharik, C. J., Foley, J. A., Delire, C., Fisher, V. A., Coe, M. T., Lenters, J. D., Young-
1246 Molling, C., Ramankutty, N., Norman, J. M., Gower, S. T.: Testing the performance of a
1247 Dynamic Global Ecosystem Model: Water balance, carbon balance, and vegetation structure.
1248 *Global biogeochemical cycles*, 14, 795-826, doi: 10.1029/1999GB001138, 2000.
1249
- 1250 Laurance, W. F. D., Fearnside, P. M., Laurance, S. G., Delamonica, P., Lovejoy, T. E.,
1251 Merona, M. R de., Chambers, Q. C., Gascon, C.: Relationship between soils and Amazon
1252 forest biomass: a landscape-scale study, *Forest Ecology Management*, 118(1-3), 127-138, doi:
1253 10.1016/S0378-1127(98)00494-0, 1999.
1254



- 1255 Laurence, W. F. D., Cochrane, M. A., Berger, S., Fearnside, P. M., Delamonica, P., Barber,
1256 C., D'angelo S., Fernandes, T.: The future of the Brazilian Amazon, *Science*, 291,
1257 438:439.doi: 10.1126/science.291.5503.438, 2001b.
- 1258 Leitão, M. M. V. B. R. Balanço de radiação em três ecossistemas da Floresta Amazônica:
1259 Campina, Campinarana e Mata densa. 157 p. Tese de doutorado (Doutorado em
1260 Meteorologia) - Instituto Nacional de Pesquisas Espaciais (INPE), São Jose dos Campos,
1261 1994.
- 1262
- 1263 Leopoldo, P. R., Franken, W., Salati, E., Ribeiro, M. N. G.: Towards a water balance in
1264 Central Amazonian region. *Experientia*, 43: 222-233. doi: 10.1007/BF01945545, 1987.
- 1265
- 1266 Leuning, R.: A critical appraisal of a combined stomatal-photosynthesis model for C3plants.
1267 *Plant, Cell and Environment*, 18, 339-355, doi: 10.1111/j.1365-3040.1995.tb00370.x, 1995.
- 1268
- 1269 Lieberman, M., Lieberman, D., Hartshorn, G. S., Peralta, R.: Small-scale altitudinal variation
1270 in lowland wet tropical forest vegetation, *Journal of Ecology*, 73 (2), 505-516, doi:
1271 10.2307/2260490, 1985.
- 1272 Linn, D. M. and Doran, J. W.: Effect of water-filled pore space on carbon dioxide and nitrous
1273 oxide production in tilled and non-tilled soils, *Soil Science Society of America Journal*,
1274 48,1267-1272, 1984.
- 1275
- 1276 Lloyd, C. R. and Marques, F. A. O.: Spatial variability of throughfall and stemflow
1277 measurements in Amazonian rainforest, *Agricultural and Forest Meteorology*, 42, 63-73, doi:
1278 10.1016/0168-1923(88)90067-6, 1988.
- 1279
- 1280 Lo, M. H., Yeh, P. J. F., Famiglietti, J. S.: Constraining water table depth simulations in a
1281 land surface model using estimated baseflow. *Advances in Water Resources*, 31 (12), 1552–
1282 1564, doi:10.1016/j.advwatres.2008.06.007, 2008.
- 1283
- 1284 Luizão, F. J. and Schubart, H. O. R.: Litter production and decomposition in a terra-firme
1285 forest of Central Amazonia. *Experientia*, 43(3), 259-265, 1987.
- 1286
- 1287 Luizão, F. J.: Litter production and mineral element input to the forest floor in a central
1288 Amazonian forest, *The Journal of Geology*, 19, 407-417, doi: 10.1007/BF00176910, 1989.
- 1289
- 1290 Luizão, R. C. C., Luizão, F. J., Paiva, R. Q., Monteiro, T. F., Souza, L. S., Kruijt, B.:
1291 Variation of carbon and nitrogen cycling processes along a topographic gradient in a central
1292 Amazonian forest, *Global Change Biology*, 22, 592-600, doi: 10.1111/j.1529-
1293 8817.2003.00757.x, 2004.
- 1294
- 1295 Lyne, V. & Hollick, M. 1979, “Stochastic time variable rainfall-runoff modelling”,
1296 Proceedings of the Hydrology and Water Resources Symposium, Perth, 10-12 September,
1297 Institution of Engineers National Conference Publication, No. 79/10, pp. 89-92.
- 1298
- 1299 Malhi, Y., Nobre, A. D., Grace, J., Kruijt, B., Pereira, M. G. P., Culf A., Scott, S.: Carbon
1300 dioxide transfer over a Central Amazonian rain forest, *Journal of Geophysical Research*, 103
1301 (24), 31593–31612, doi: 10.1029/98JD02647, 1998.
- 1302
- 1303 Malhi, Y., Baldocchi, D. D., Jarvis, P. G.: The carbon balance of tropical, temperate and
1304 boreal forests, *Plant Cell Environ* 22(6), 715-740, 1999.



- 1305
1306 Malhi, Y., Phillips, O. L., Baker, T., Wright, J., Almeida, S., Arroyo, L., Frederiksen, T.,
1307 Grace, J., Higuchi, N., Killeen, T., Laurance, W. F., Leão, C., Meir, P., Monteagudo, A.,
1308 Neill, D., Núñez Vargas, P., Panfil, S. N., Patiño, S., Pitman, N., Quesada, C. A., Ruelas-LI, A.,
1309 Salomão, R., Saleska, S., Silva, N., Silveira, M., Sombroek, W. G., Valencia, R., Vásquez
1310 Martínez, R., Vieira, I. C. G., Vicenti, B.: An international network to understand the biomass
1311 and dynamics of Amazonian forests (RAINFOR), *Journal of Vegetation Science*, 13, 439–
1312 450, doi: 10.1111/j.1654-1103.2002.tb02068.x, 2002.
- 1313
1314 Malhi, Y., Baker, T. R., Phillips, O. L., Almeida, S., Alvarez, E., Arroyo, L., Chave,
1315 J., Czimczik, C. I., Di Fiore, A., Higuchi, N., Killeen, T. J., Laurance, S. G., Laurance, W. F.,
1316 Lewis, S. L., Montoya, L. M. M., Monteagudo, A., Neill, D. A., Vargas, P. N., Patiño, S.,
1317 Pitman, N. C. A., Quesada, C. A., Salomao, R., Silva, J. N. M., Lezama, A. T., Martínez, R.
1318 V., Terborgh, J., Vinceti, B., Lloyd, J.: The above-ground coarse wood productivity of 104
1319 Neotropical forest plots, *Global Change Biology*, 10, 563–591, doi: 10.1111/j.1529-
1320 8817.2003.00778.x, 2004.
- 1321
1322 Malhi, Y., Wood, D., Baker, T. R., Wright, J., Phillips, O. L., Cochrane, T., Meir, P., Chave,
1323 J., Almeida, S., Arroyo, L., Higuchi, N., Killeen, T. J., Laurence, A. G., Laurence, W. F.,
1324 Lewis, S. L., Monteagudo, A., Neill, D. A., Núñez Vargas, P., Pitman, N. C. A., Quesada, C. A.,
1325 Salomão, R., Silva, J. N. M., Lezama, A. T., Terborgh, J., Vásquez Martínez, R., Vicenti, B.:
1326 The regional variation of aboveground live biomass in old-growth Amazonian forests, *Global
1327 Change Biology*, 12, 1107–1138, doi: 10.1111/j.1365-2486.2006.01120.x, 2006.
- 1328
1329 Malhi, Y., Aragao, L. E. O. C., Metcalfe, D. B., Paiva, R., Quesada, C. A., Almeida, S.,
1330 Anderson, L., Brando, P., Chambers, J. Q., da Costa, A. C. L., Hutyra, L. R., Oliveira, P.,
1331 Patiño, S., Pyle, E. H., Robertson, A. L., Teixeira, L. M.: Comprehensive assessment of
1332 carbon productivity, allocation and storage in three Amazonian forests, *Global Change
1333 Biology*, 15, 1255–1274, doi.org/10.1111/j.1365-2486.2008.01780.x, 2009b.
- 1334
1335 Marengo, J. A.: Interdecadal variability and trends of rainfall across the Amazon basin,
1336 *Theoretical and Applied Climatology*, 78, 79–96, doi: 10.1007/s00704-004-0045-8, 2004.
- 1337
1338 Marengo, J. A., Nobre, C. A., Tomasella, J., Oyama, M. D., de Oliveira, G. S., de Oliveira,
1339 R., Camargo, H., Alves, L. M., Brown, I. F.: The drought of Amazônia in 2005, *Journal of
1340 Climate*, 21, 495–516. doi: 10.1175/2007JCLI1600.1, 2008.
- 1341
1342 Marques Filho, A. O., Dallarosa, R. G., Pacheco, V. B.: Radiação solar e distribuição vertical
1343 de área foliar em floresta- Reserva Biológica do Cuieiras- ZF2, Manaus, *Acta Amazônica*, 35
1344 (4), 427–436, doi.org/10.1590/S0044-59672005000400007, 2005.
- 1345
1346 Marques, J. D. O.: Influência de atributos físicos e hídricos do solo na dinâmica do carbono
1347 orgânico sob diferentes coberturas vegetais na Amazônia Central. Tese de doutorado. Instituto
1348 Nacional de Pesquisas da Amazônia/Universidade Federal da Amazônia, Manaus, Amazônia.
1349 277pp, 2009.
- 1350
1351 Metcalfe, D., Meir, P., Williams, M.: A comparison of methods for converting rhizotron root
1352 length measurements into estimates of root mass production per unit ground area, *Plant Soil*,
1353 301, 279–288, doi: 10.1007/s11104-007-9447-6, 2007.
- 1354



- 1355 Miguez-Macho, G. and Fan, Y.: The role of groundwater in the Amazon water cycle: 2.
1356 Influence on seasonal soil moisture and evapotranspiration, *Journal Geophysical Research*,
1357 117, D15114, doi: 10.1029/2012JD017540, 2012.
1358
- 1359 Miller, S. D., Goulden, M. L., Menton, M. C., da Rocha, H. R., de Freitas, H. C., Figueira, A.
1360 M. E. S., de Sousa, C. A. D.: Biometric and micrometeorological measurements of tropical
1361 forest carbon balance, *Ecological Applications*, 14 (4), 114-126, doi: 10.1890/02-6005, 2004.
1362
- 1363 Monteith, J. L.: *Evaporation and Environment*. 19th Symposia of the Society for
1364 Experimental Biology, University Press, Cambridge, 19:205-234, 1965.
1365
- 1366 Moraes, J. M., Schuler, A. E., Dunne, T., Figueiredo, R. O., Victoria, R.: Water storage and
1367 runoff processes in plinthic soils under forest and pasture in Eastern Amazonia. *Hydrological*
1368 *Processes* 20: 2509-2526. doi: 10.1002/hyp.6213, 2006.
1369
- 1370 Nathan, R. J., McMahon, T.: Evaluation of automated techniques for baseflow and recessi on
1371 analyses, *Water Resources Research*, 26(7), 1465-1473, doi: 10.1029/WR026i007p01465,
1372 1990.
1373
- 1374 Nobre, A. D.: *Relação entre Matéria Orgânica e Mineral de uma topossequência Latossolo-*
1375 *Podzol e a Cobertura de Floresta Tropical Úmida na Bacia do Rio Curiaú, Amazônia Central.*
1376 *Dissertação de Mestrado INPA-FUA, Manaus, Amazônia.* 133p, 1989.
1377
- 1378 Nobre, A. D., Cuartas, L. A., Hodnett, M. G., Rennó, C. D., Rodrigues, G., Silveira, A.;
1379 Waterloo, M.; Saleska, S.: Height Above the Nearest Drainage - a hydrologically relevant
1380 new terrain model, *Journal of Hydrology*, 404, 13-29, doi:10.1016/j.jhydrol.2011.03.051, 2011.
1381
- 1382 Noilhan, J. and Mahfouf J. F.: The ISBA land surface parameterization scheme, *Global and*
1383 *Planetary Change*, 13, 145 – 159, 1996.
1384
- 1385 Nortcliff, S. and Thornes, J. B.: Seasonal variations in the hydrology of a small forested
1386 catchment near Manaus, Amazonas, and the implications for its management. In: Lal, R.;
1387 Russel, E.W. (eds) *Tropical Agricultural Hydrology*. Wiley, New York, USA, 1981.
1388
- 1389 Oberbauer, S. F., Gillespie, C. T., Cheng, W., Gebauer, R., Sala Serra, A., Tenhunen J. D.:
1390 Environmental effects on CO₂ efflux from riparian tundra in the northern foothills of the
1391 Brooks Range, Alaska, U.S.A, *Oecologia*, 92, 568-577, doi: 10.1007/BF00317851, 1992.
1392
- 1393 Ohtaki, E.: Application of an infrared carbon dioxide and humidity instrument to studies of
1394 turbulent transport, *Boundary-Layer Meteorology*, 29, 85-107, doi: 10.1007/BF0011912,
1395 1984.
1396
- 1397 Oliveira, A. N., Amaral, I. L., Nobre, A. D., Couto, L. B., Sato, R. M., Santos, J. L., Ramos,
1398 J.: Composição e diversidade florística de uma floresta ombrófila densa de terra firme na
1399 Amazônia central, Amazonas, Brasil. II LBA Scientific Conference, Manaus. 42pp, 2002.
1400
- 1401 Oliveira, A. N., Amaral, I. L.: Florística e fitossociologia de uma floresta de
1402 vertente na Amazônia Central, Amazonas, Brasil, *Acta Amazônica*, 34 (1), 21–34,
1403 doi.org/10.1590/S0044-59672004000100004, 2004.
1404



- 1405 Oliveira, M. B. L.: Estudo das trocas de energia sobre a floresta amazônica. 144 p. Tese de
1406 Doutorado (Doutorado em Ciências de Florestas Tropicais) - Instituto Nacional de Pesquisas
1407 da Amazônia (INPA), Amazônia, 2010.
1408
- 1409 Pan, Y., Birdsey, R. A., Fang, J., Houghton, R., Kauppi, P. E., Kurz, W. A., Phillips, O. L.,
1410 Shvidenko, A., Lewis, S.L., Canadell, J. G., Ciais, J., Jackson, R. B., Pacala, S. W., McGuire,
1411 A. D., Piao, S., Rautiainen, A., Sitch S., Hayes D. A.: Large and Persistent Carbon Sink in
1412 theWorld's Forests, *Science*, 333, 988-993, doi: 10.1126/science.1201609, 2001.
1413
- 1414 Pelissier, P., Dray, S., Sabatier, D.: Within-plot relationships between tree species occurrences
1415 and hydrological soil constraints: na exemple in French Guiana investigated trough canonical
1416 correlation analysis, *Plant Ecology*, 162 (2), 143-156, doi:10.1023/A:1020399603500, 2001.
1417
- 1418 Pezeshki, S. R. and DeLaune R. D.: Soil Oxidation-Reduction in wetlands and its impact on
1419 plant functioning, *Biology*, 1, 196-221, doi:10.3390/biology1020196, 2012.
1420
- 1421 Pinheiro, T. F.: pp111. Caracterização e estimativa de biomassa em fitofisionomias de
1422 Terra-firme da Amazônia Central por inventário florístico e por textura de
1423 imagens simulação do MAPSAR (Multi-Application Purpose SAR). Dissertação
1424 (mestrado em Sensoriamento Remoto) - Instituto Nacional de Pesquisas
1425 Espaciais (INPE), São José dos Campos, 2007.
1426
- 1427 Pollard, D. and Thompson, S. L. Use of a land-surface-transfer scheme (LSX) in a global
1428 climate model: the response to doubling stomatal resistance, *Global and Planetary Change*,
1429 10, 129-161, doi:10.1016/0921-8181(94)00023-7, 1995.
1430
- 1431 Prance, G. T.: American Tropical Forests. In: Lieth H, Werger MJA. (eds). Tropical Rain
1432 Forest Ecosystems. Ecosystems of the World 14B, *Elsevier Plub*, Amsterdam, 99-132, 1989.
1433
- 1434 Pyle, E. H., Santoni, G. W., Nascimento, H. E. M., Hutyra, L. R., Vieira, S., Curran, D. J., van
1435 Haren, J., Saleska, S. R., Chow, V.Y., Camargo, P. B., Laurance, W. F., Wofsy, S. C.:
1436 Dynamics of carbon, biomass, and structure in two Amazonian forests, *Journal of*
1437 *Geophysical Research*, 113, G00B08, doi: 10.1029/2007JG000592, 2008.
1438
- 1439 Ranzani, G.: Identificação e caracterização de alguns solos da Estação Experimental de
1440 Silvicultura Tropical do INPA, *Acta Amazônica*, 10, 7-41, 1980.
1441
- 1442 Rawls, W. J., Brakensiek, D. L., Saxton, K. E.: Estimation of soil water properties,
1443 *Transactions of the ASAE*, 25, 1316-1330, 1982.
1444
- 1445 Rennó, C. D., Nobre, A. D., Cuartas, L. A., Soares, J. V., Hodnett, M. G., Tomasella, J.,
1446 Waterloo, M. J.: HAND, a new terrain descriptor using SRTM-DEM: mapping terra-firme
1447 rainforest environments in Amazonia, *Remote Sensing of Environment*, 112, 3469-3481, doi:
1448 10.1016/j.rse.2008.03.018, 2008.
1449
- 1450 Ribeiro, J. E. L. S., Hopkins, M. J. G., Vicentini, A., Sothers, C. A., Costa, M. A. S., Brito, J.
1451 M., Souza, M. A. D., Martins, L. H. P., Lohmann, L. G., Assunção, P. A. C. L., Pereira, E. C.,
1452 Silva, C. F., Mesquita, M. R., Procópio, L. C.: Flora da Reserva Ducke: Guia de identificação
1453 das plantas vasculares de uma floresta de terra firme na Amazônia Central. Manaus, INPA.
1454 816pp, 1999.



- 1455
1456 Shuttleworth, W. J.; Gash, J. W. C.; Lloyd, C. R.; McNeil, D. D.; Moore, C. J.; Wallace, J. S.:
1457 An integrated micrometeorological system for evaporation measurement, *Agricultural*
1458 *and Forest Meteorology*, 43, 295-317, doi:10.1016/0168-1923(88)90056-1, 1988.
1459
1460 Shuttleworth, W. J.: Micrometeorology of temperate and tropical forest. *Philos,*
1461 *Trans.Roy.Soc.London*, B324, 299-334, 1989.
1462
1463 Silva, R. P.: Alometria, estoque e dinâmica da biomassa de florestas primárias e secundárias
1464 na região de Manaus (AM). Ph.D. Dissertation, Universidade Federal do Amazonas, Manaus,
1465 Brazil, p 152 (in Portuguese with English abstract), 2007.
1466
1467 Sotta, E. D., Meir, P., Malhi, Y., Nobre, A. D. Grace, J.: Soil CO₂ efflux in a tropical forest
1468 in the central Amazon, *Global Change Biology*, 10, 601–617, doi:10.1111/j.1529-
1469 8817.2003.00761.x, 2004.
1470
1471 Souza, J. S. Dinâmica espacial e temporal do fluxo de CO₂ do solo em floresta de
1472 terra firme na Amazônia Central. Master's thesis, Instituto Nacional de Pesquisas
1473 da Amazonia and Universidade Federal do Amazonas, Manaus, Amazonas State,
1474 Brazil, 2004.
1475
1476 Takyu, M., Aiba, S., Kitayama, K.: Effects of topography on tropical lower montane forests
1477 under different geological conditions on Mount Kinabalu, Borneo, *Plant Ecology*, 159:35-49,
1478 doi:10.1023/A:1015512400074, 2002.
1479
1480 Tomasella, J. and Hodnett, M.G.: Soil hydraulic properties and van Genuchten parameters
1481 for an oxisol under pasture in central Amazonia. In *Amazonian Deforestation and Climate*,
1482 Gash JHC, Nobre CA, Roberts JM, Victoria RL (eds). John Wiley and Sons: West Sussex,
1483 101-124, 1996.
1484
1485 Tomasella, J., Hodnett, M. G., Cuartas, L. A., Nobre, A. D., Waterloo, J., Oliveira, S. M.: The
1486 water balance of an Amazonia microcatchment: the effect of interannual variability of rainfall
1487 on hydrological behaviour. *Hydrological Processes*, 22, 2133-2147, doi: 10.1002/hyp.6813,
1488 2008.
1489
1490 Tomasella, J., Borma, L. S., Marengo, A., Rodriguez, D. A., Cuartas, L. A., Nobre, C. A.,
1491 Prado M. C. R.: The droughts of 1996-1997 and 2004-2005 in Amazonia: hydrological
1492 response in the river main-stem, *Hydrological Process*, 25, 1228-1242, doi:
1493 10.1002/hyp.7889, 2010.
1494
1495 Tota, J., Fitzjarrald, D. R., Staebler, R. M., Sakai, R. K., Moraes, O.M. M., Acevedo, O. C.,
1496 Wofsy, S. C., and Manzi, A. O.: Amazon rain forest subcanopy flow and the carbon budget:
1497 Santarém LBA-ECO site, *Journal of Geophysical Research: Biogeosciences*, 113(15),
1498 G00B02, doi:10.1029/2007JG000597, 2008.
1499
1500 Twine, T. E., Kustas, W. P., Norman, J. M., Cook, D. R., Houser, P. R., Meyers, T. P.,
1501 Prueger, J. H., Starks, P. J., Wesely, M. L.: Correcting eddy-covariance flux underestimates
1502 over a grassland, *Agricultural and Forest Meteorology*, 103, 279-300, 2000.
1503



- 1504 Varejão, E. V. V., Bellato, C. R., Fontes, M. P. F., Mello, J. W. V.: Arsenic and trace metals
1505 in river water and sediments from the southeast portion of the Iron Quadrangle, Brazil.
1506 Environmental Monitoring and Assessment. 172 (1), 631–642. doi: 10.1007/s10661-010-
1507 1361-3, 2011.
- 1508
- 1509 Vieira, S., de Camargo, P. B., Selhorst, D., da Silva, R., Hutyra, L., Chambers, J. Q., Brown,
1510 I. F., Higuchi, N., dos Santos, J., Wofsy, S. C., Trumbore, S. E., Martinelli, L. A.: Forest
1511 structure and carbon dynamics in Amazonian tropical rain forests. *Oecologia*, 140: 468-479.
1512 doi:10.1007/s00442-004-1598-z, 2004.
- 1513
- 1514 Verhoef, A. and Egea, G.: Modeling plant transpiration under limited soil water: Comparison
1515 of different plant and soil 25 hydraulic parameterizations and preliminary implications for
1516 their use in land surface models, *Agricultural and Forest Meteorology*, 191, 22-32, doi:
1517 10.1016/j.agrformet.2014.02.009 2014.
- 1518
- 1519 Von Randow, C., Manzi, A. O., Kruijt, B., de Oliveira, P. J., Zanchi, F. B., Silva, R. L.,
1520 Hodnett, M. G., Gash, J. H. C., Elbers, J. A., Waterloo, M.J., Cardoso, F.L, Kabat,
1521 P.:Comparative measurements and seasonal variations in energy and carbon exchange over
1522 forest and pasture in southwest Amazonia, *Theoretical and Applied Climatology*,
1523 doi:10.1007/s00704-004-0041-z, 2004.
- 1524
- 1525 Waterloo, M. J., Oliveira, S. M., Drucker, D. P., Nobre, A. D., Cuartas L. A., Hodnett, M. G.,
1526 Langedijk, I., Jans, W. W. P., Tomasella, J., de Araújo A. C., Pimentel, T. P., Múnera J. C.:
1527 Export of organic carbon in runoff from an Amazonian blackwater catchment, *Hidrological*
1528 *Processes*, 20, 2581-2597, doi: 10.1002/hyp.6217, 2006.
- 1529
- 1530 Wilson, K., Goldstein, A., Falge, E., Aubinet, M., Baldocchi, D., Berbigier, P., Bernhofer, C.,
1531 Ceulemans, R., Dolman, H., Field, C., Grelle, A., Ibrom, A., Law, B. E., Kowalski, A.,
1532 Meyers, T., Moncrieff, J., Monson, R., Oechel, W., Tenhunen, R. V., Shashi, V.: Energy
1533 balance closure at FLUXNET sites, *Agricultural and Forest Meteorology*, 113(1–4), 223-243,
1534 doi.org/10.1016/S0168-1923(02)00109-0, 2002.
- 1535
- 1536 Yeh, P. J. F. and E. A. B. Eltahir.: Representation of water table dynamics in a land surface
1537 scheme: Model development. *Journal Climatology*, 18, 1861–1880, doi: 10.1175/JCLI3330.1,
1538 2005a.
- 1539
- 1540 Yeh, P. J. F. and E. A. B. Eltahir.: Representation of water table dynamics in a land surface
1541 scheme: Subgrid variability. *Journal Climatology*, 18, 1881–1901, doi: 10.1175/JCLI3331.1,
1542 2005b.
- 1543
- 1544 Zanchi, F. B.: Vulnerability to drought and soil carbon exchange of valley forest in Central
1545 Amazonia - Brazil. 2013. 186 p. Tese de doutorado (Doutorado em Ciências Geoambientais) -
1546 Free University of Amsterdam, Holanda, 2013.
- 1547
- 1548 Zanchi, F. B., Meesters, A. G. C. A., Waterloo, J. M., Kruijt, B., Kesselmeier, J., Luizão, F.
1549 L., Dolman, A. J.: Soil CO₂ exchange in seven pristine Amazonian rain forest sites in
1550 relation to soil temperature, *Agricultural and Forest Meteorology*, 192-193, 96-107,
1551 doi:10.1016/j.agrformet.2014.03.009, 2014.
- 1552



- 1553 Zarin, D. J., Ducey, M. J., Tucker, J. M., Salas, W. A.: Potential biomass accumulation in
1554 Amazonian regrowth forests, *Ecosystems*, 4 (7), 658–668, doi: 10.1007/s10021-001-0035-y,
1555 2001.
1556
1557 Zha, T. S., Barr, A. G., Bernier, P. Y., Lavigne, M. B., Trofymow, J. A., Amiro, B. D., Arain,
1558 M.A., Bhatti, J. S., Black, T. A., Margolis, H. A., McCaughey, J. H., Xing, Z. S., Van Rees,
1559 K. C. J., Coursolle, C.: Gross and aboveground net primary production at Canadian forest
1560 carbon flux sites, *Agricultural and Forest Meteorology*, 174-175, 54–64, doi:
1561 10.1016/j.agrformet.2013.02.004, 2013.
1562